Journal Name

ARTICLE

Colloidal Semiconductor Nanocrystals in Energy Transfer Reactions

Received 00th January 20xx,
Accepted 00th January 20xx

DOI: 10.1039/x0xx00000x

www.rsc.org/

Pavel Moroz, [a,b] Luis Royo Romero, [a] and Mikhail Zamkov *[a,b]

Excitonic energy transfer is a versatile mechanism by which colloidal semiconductor nanocrystals can interact with a variety of nanoscale species. While this process is analogous to dipole-dipole coupling in molecular systems, the corresponding energy transfer dynamics can deviate from that of molecular assemblies due to manifestations of bulk-like features in semiconductor colloids. In particular, weak exciton binging, small single-triplet exciton splitting, and the energy disorder across nanocrystal ensembles can all play a distinctive role in the character of ensuing energy conversion processes. To characterize the variety of energy transfer schemes involving nanocrystals, this feature article will discuss the latest research both from our and other groups on the key scenarios under which nanocrystals can engage in the energy transfer with other nanoparticles, organic fluorophores, and plasmonic nanostructures, highlighting potential technological benefits to be gained from such processes. We will also shed light on experimental strategies for probing the energy transfer in nanocrystals-based assemblies with a particular emphasis on novel characterization techniques.

Introduction

The energy flow across most quantum-confined systems proceeds *via* the transfer of electrically neutral excitons, which contrasts the charge-mediated energy transfer in bulk semiconductors. Examples of the excitonic energy transfer (ET) in nanoscale systems can be found in many biological and poly-molecular materials. For instance, cascade-like ET is the first step of the energy conversion during photosynthesis[1] and is the primary process of the energy flow in excitonic solids[2-4] and organic crystals.[5] Diffusive energy transport is also pervasive in living tissues and proteins, where excitons are transmitted tens of angstroms away from single-site excitations.[6,7]

Colloidal semiconductor nanocrystals (NC) represent a well-known example of artificial systems that support the excitonic energy transfer. These materials can engage in a variety of ET processes with other nanoscale partners, including organic molecules, metal nanostructures, and other quantum confined semiconductors (Fig. 1). These energy-transfer systems hold strong promise for the development of new paradigms for solar energy production, solid state lighting, sensing, and near-field optical imaging applications, which will be discussed in depth. We will also highlight the experimental strategies for probing the energy transfer in nanocrystals-based assemblies with a particular emphasis on novel characterization techniques.

One of the well-known energy transfer platforms involving semiconductor NCs represents an assembly of semiconductor nanoparticles and surface-anchored molecules.[8-10] The energy exchange in such assemblies modulates the photoluminescence (PL) intensity of the donor moiety, providing a general paradigm for applications in biosensing.[10-15] On the other hand, the photoinduced charge separation at the nanoparticle-dye interface makes these assemblies attractive candidates for the development of light-harvesting materials.[16-18] Semiconductor nanocrystals have also been shown to engage in the photoinduced energy transfer with proximal metal nanoparticles. In this case, the near-field interaction between electric dipoles of a semiconductor nanocrystal and a localized surface plasmon can lead to the bilateral transfer of the excitation energy. Such metal-semiconductor energy exchange offers several opportunities for energy conversion on nanoscale. For instance, plasmon-induced quenching of the semiconductor PL represents a popular biosensing strategy,[19-21] while, the plasmon-enhanced absorption in semiconductors can be used to increase the optical extinction of photocatalytic and photovoltaic absorbers.[22-24] When processed into solids, semiconductor nanocrystals can engage in the energy transfer with other quantum confined semiconductors.[25-27] Similar to organic crystals, the energy transfer across close-coupled nanocrystal assemblies is mediated by the exciton diffusion, which rate is tunable through the use of interparticle binding motifs. The diffusion of energy in light-emitting nanocrystal solids is typically restricted to a small volume in order to prevent exciton migration towards luminescence-quenching boundaries.[28-36] Conversely, the excitons diffusion to charge-separating interfaces is vastly beneficial for nanocrystal solar cells, where it leads to photocurrent generation.[35,37-49]

[a] *Department of Physics and Astronomy, Bowling Green State University, Bowling Green, Ohio 43403, United States.*
[b] *The Center for Photochemical Sciences, Bowling Green State University, Bowling Green, Ohio 43403, United States.*
Electronic Supplementary Information (ESI) available: [details of any supplementary information available should be included here]. See DOI: 10.1039/x0xx00000x

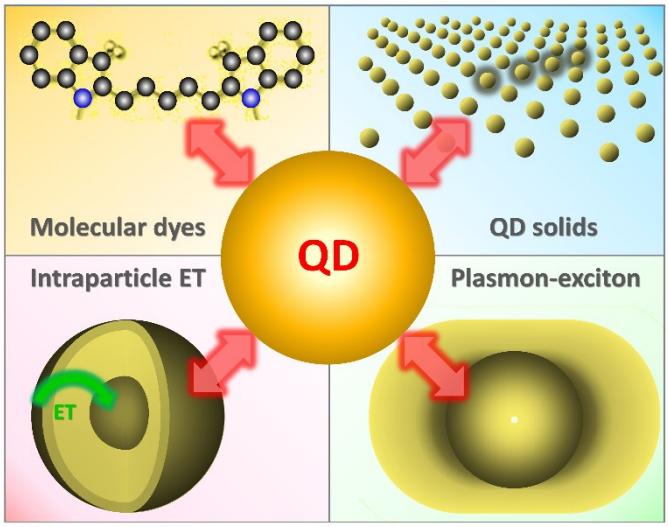

Figure 1. Possible mechanisms of excitonic energy transfer involving semiconductor nanocrystals.

Energy transfer in solids of semiconductor nanocrystals

The dynamics of energy flow in nanocrystal solids represents an intricate combination of bulk and molecular characteristics. While the energy transport across nanocrystal assemblies is excitonic in nature, there is usually a significant driving force for an electron-hole dissociation into a pair of free charges (Fig. 2). Such a high probability of exciton dissociation is characteristic of semiconductor nanocrystals and is a direct result of a large quantum confinement volume, which leads to weak exciton binding.[50] In this regime, the splitting of bound electron-hole pairs can be triggered by low-energy processes, such as charge tunneling between neighboring nanocrystals.[51] The resulting ET dynamics is therefore different from both the molecular films, where excitons dissociate primarily at phase boundaries and bulk materials, where electron-hole binding energy is usually negligible. One of the benefits of such weakly bound excitons lies in the ability to control the exciton dissociation probability, p_{diss}, through the use of different nanoparticle binding motifs. This strategy allows tuning electronic properties of nanocrystal solids between those of molecular films (low p_{diss}) and bulk materials (high p_{diss}).

A rapid dissociation of excitons in nanocrystal solids is generally desirable for applications that benefit from the photoinduced charge separation. In this case, the dissociation represents the conversion of the optical energy into the electrical potential of separated charges ($\hbar\omega \rightarrow$ eV), which is required for the operation of photoelectrochemical cells, photodetectors, and solar cell devices.[47,52-56] In these applications, the exciton dissociation probability is usually enhanced through the use of short-length interparticle linkers, such as EDT or 3-mercaptopropionic acid (MPA), [53,54,57-60] which increase the charge tunneling rate. From the standpoint of photovoltaic performance, the fast dissociation of excitons can reduce the probability of their radiative recombination, thereby enhancing the overall charge extraction efficiency; meanwhile, the corresponding reduction in the exciton diffusion volume will help minimizing exciton trapping at potential energy minima associated with larger nanocrystals in the film.

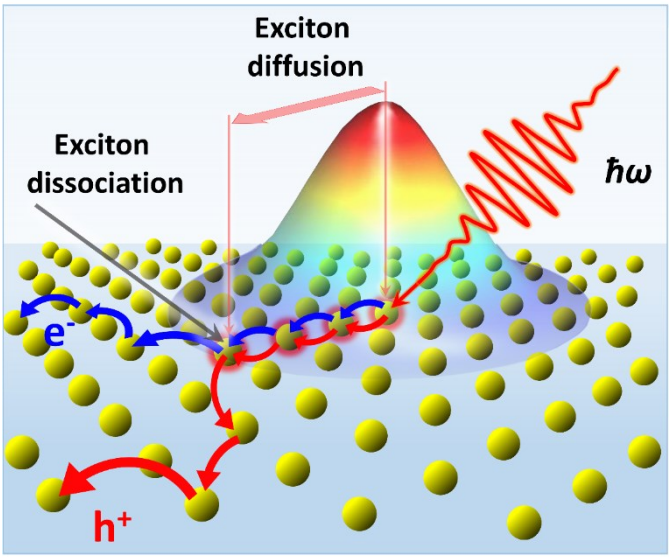

Figure 2. Photoinduced energy conversion in nanocrystal solids. The photon absorption results in the formation of localized excitons that diffuse through a film at a rate determined by the strength of the interparticle coupling. Similar to polymer films, a singlet exciton “hops" through the thermally accessible energy landscape towards the potential energy minimum. The subsequent decay of excitons is then driven by their recombination (radiative or non-radiative) or dissociation into a free electron-hole pair. Adapted from Ref.61. Copyright 2015 American Chemical Society.

Nanocrystals solids featuring a low exciton dissociation probability are generally preferred in light-emitting applications, where the radiative recombination of electron-hole pairs is beneficial to the device performance. In this case, the probability of exciton dissociation can be reduced through the use of long-chain interparticle linkers that decrease the charge transfer coupling between nanoparticles (see Fig. 3a). For instance, *Sun et al.* has demonstrated that the electroluminescence intensity of PbS NC solids increases proportionally to the lengths of the linker molecule.[30] When the dot-to-dot spacing in the emissive layer was augmented from three to eight CH_2 groups, the efficiency grew by a factor of 150. The steady state PL of nanocrystals solids was shown to follow the same trend. For example, the PL lifetime of 8-mercaptooctanoic acid (MOA)-linked PbS NC films featuring 1.7-nm interparticle distances was found to be 14 times greater than that of MPA-linked PbS NC films featuring a 0.9-nm gap.[61] The increased PL of MOA-linked solids was ascribed to the reduced charge transfer rate in weakly coupled PbS NCs.

As an alternative to tuning the interparticle nanoparticle binding motif, the PL of nanocrystal solids can be increased by incorporating nanocrystals within an inorganic matrix of wider band gap materials. As was demonstrated by Kovalenko *et al*.,[62] light-emitting PbS NC solids could be fabricated by the encapsulation of nanoparticles within metal chalcogenide complexes (MCC).[63-65] This methodology relied on sintering of hybrid MCCs ligands into As_2S_3 amorphous matrices, which gave rise to an all-inorganic film architecture exhibiting a stable IR emission. The high dielectric constant of the As_2S_3 medium also permitted fast radiative rates in otherwise "slow" PbS NCs. In addition to chalcogenide glasses, perovskite-based matrices have also been used to encapsulate semiconductor nanocrystals leading to near-IR emitting devices with quantum efficiencies exceeding 2%.[66] In another study,[34] the assembly of emissive nanocrystal films has been achieved by using the semiconductor matrix embedded nanocrystal array (SMENA) approach,[46,67] which benefited from heteroepitaxial bonds between nanocrystals and all-inorganic matrices of a wider gap semiconductor. For instance, SMENA-processed solids of CdSe and PbS nanocrystals utilizing CdS matrices have given rise to the PL quantum yield of 52% and 3%, respectively.[33,34]

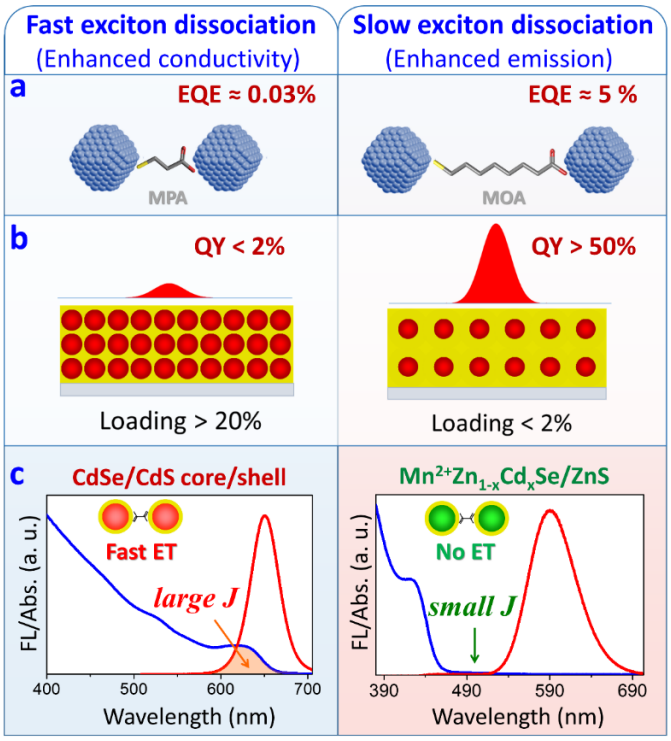

Figure 3. Experimental strategies for tuning the exciton dissociation probability in nanocrystal solids. (a). Long-chain interparticle linkers suppress the exciton dissociation and improve the emission quantum yield of nanoparticle solids. Conversely, short-chain linkers enhance the exciton dissociation rate. (b). The exciton dissociation probability of matrix-encapsulated nanocrystals is inversely proportional to the interparticle distance, which allows tuning the solid properties between light-harvesting (left) and light-emitting (right). (c). The exciton dissociation probability can be controlled *via* the donor-acceptor spectral overlap, *J*. Nanocrystal solids featuring a lower *J* exhibit a lower rate of the interparticle energy transfer, which reduces the corresponding exciton diffusion volume. As a result, the probability of an exciton reaching emission-quenching defects diminishes, enhancing the emission. An inverse correlation between exciton diffusion rates and the overlap integral *J* is shown through a comparison of CdSe/CdS and Mn^{2+}-doped $Zn_{1-x}Cd_xSe/ZnS$ NC solids. Owing to a vanishing absorption-emission overlap in Mn^{2+}-doped nanocrystals, the corresponding *J* integral is 10^5 times smaller than that of CdSe/CdS films, which was manifested by a much slower exciton diffusion (hopping time ≈ 0.3 ms) and a strongly suppressed exciton dissociation in Mn^{2+}-doped $Zn_{1-x}Cd_xSe/ZnS$ NC solids.

Increasing the distance between nanocrystals in a solid does not always represent the optimal strategy for improving the PL characteristics of light-emitting devices. For instance, tuning the size of interparticle linkers in a nanoparticle film enables a fairly predictive control over exciton diffusion rates, but doesn't offer a reliable scheme for regulating the spatial extent of exciton diffusion. A large diffusion volume can cause the excitation energy to reach luminescent quenching boundaries, which is potentially detrimental for LED applications. One promising strategy for reducing the diffusion volume relies on lowering the absorption-emission spectral overlap between nanocrystals, *J*. It was recently demonstrated that solids featuring a low *J* exhibit an intrinsically slower exciton diffusion (Fig. 3c). Even in solids featuring short interparticle linkers (e.g. oxalic acid), a relatively low diffusivity could be achieved for type II or transition-metal-doped nanoparticles that tend to exhibit a low *J* value. Assemblies of these colloids foster a desirable combination of short interparticle distances and slow energy diffusion (high brightness), which is crucial for the development of light-emitting applications. For instance, the exciton diffusivity of Mn^{2+}-doped $Zn_{1-x}Cd_xSe/ZnS$ was found to be 10^5 times lower than in CdSe/CdS NC films (Fig. 3c) allowing these films to retain its solution emission QY.[68]

An uneven energy landscape represents another distinctive aspect of the energy transfer in nanocrystal solids. Owing to inhomogeneous broadening of nanocrystal sizes, the corresponding dispersion of exciton energies in colloidal assemblies could be comparable to the room temperature kT. Under these conditions, excitons are likely to be trapped at local minima of the potential energy, which effectively shortens their diffusion lengths. The presence of such "deep" energetic traps in nanocrystal films distinguishes them from polymer and molecular assemblies, where exciton energy variations across molecular subunits are considerably smaller.

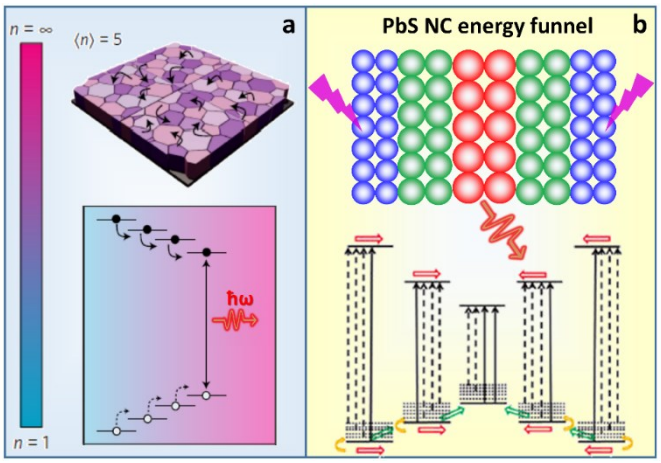

Figure 4. (a). The process of energy funneling in perovskite nanocrystals.[72] An assembly of quantum-size-tuned $CH_3NH_3PbI_3$ grains was used to funnel photoexcitations to the lowest-bandgap light-emitter, enabling an external quantum efficiency of 8.8% in the near infrared (IR). Reproduced with permission from ref. 72. Copyright 2016 Springer Nature Publishing. (b). An illustration of the exciton funneling strategy, which is designed to concentrate the energy of small-diameter PbS NCs *via* a transfer to the sublayer of large-diameter PbS NCs. Adapted with permission from ref. 70. Copyright 2011 American Chemical Society.

The energy disorder exceeding room temperature kT is generally unfavorable for photovoltaic applications of nanocrystal films, as the energy of trapped excitons is typically lost to the radiative recombination or non-radiative decay. Conversely, the presence of excitonic traps could be quite beneficial to the performance of quantum dot light emitting materials.[31] The local minima of the potential energy corresponding to large-diameter nanocrystals could be strategically placed within a nanoparticle solid to serve as emissive sites. In this case, the diffusion of excitons from small to large species will allow concentrating the excitation energy within the light-emitting layer.[69,70] This idea was exemplified in a recent work,[70] where a cascade-like energy transfer across ascending diameter nanoparticle layers was used to enhance the infrared-range emission of PbS solids (Fig. 4b). Here, the transport of excitons along the energy gradient of mixed-diameter PbS films (assembled with 1,3-benzenedithiol linkers) has resulted in a 19-fold improvement in the emission of acceptor nanocrystals. A similar mechanism of energy concentration was demonstrated in assemblies of $CsPbBr_3$ perovskite nanocrystals[71] as well as in perovskite light-emitting diodes[72] developed from a series of differently quantum-size-tuned grains of $CH_3NH_3PbI_3$. The resulting LED architecture funneled photoexcitations to the lowest-bandgap light-emitter, enabling an external quantum efficiency of 8.8% in the near infrared. The principle of energy funneling towards the potential minimum of nanocrystal solids was also demonstrated as the light concentration mechanism in photovoltaic devices. Despite the fact that stable excitons are generally unfavorable for the solar cell performance, layers of descending-diameter PbS nanocrystals have been used for concentrating the photoinduced energy within the charge-separating domain.[73]

The ability of nanocrystal solids to funnel the photoinduced energy into acceptor nanoparticles can be harnessed towards multiple exciton generation (MEG). The MEG phenomenon in semiconductor nanocrystals in potentially beneficial to a number of applications, including quantum dot lasers,[74-76] where the light amplification requires multiple excited carriers, or photoelectrochemical cells,[77,78] where catalytic processes often involve several photoinduced charges (e.g. H_2 generation). The challenging aspect of utilizing multiple excitations in semiconductor nanocrystals lies in the ability to suppress their non-radiative Auger recombination.[75] With the inverse volume dependence of Auger decay rates,[79] the general solution for increasing the lifetime of biexcitons is often sought in nanoparticle geometries that allow for a larger excitonic volume. Along these lines, zero-dimensional semiconductors have given way to architectures featuring a mixed dimensionality, such as alloyed core/shell nanoparticles,[80,81] nanorod-shaped heterostructures,[82-85] and nanoplatelets (NPLs).[86-90]

Semiconductor nanoshells[91-93] represent another viable nanoscale geometry for concentrating multiple excitons. In these nanostructures, the excitonic layer is grown in form of a shell on the surface of a bulk-size core domain (Fig. 5a-e). The ensuing energy gradient gives rise to two-dimensional excitations that reside primarily in the shell and, therefore, preserve the radial confinement of carriers, regardless of the particle size. The existence of shell-confined excitons was recently demonstrated in CdS/CdSe core/shell quantum dots (QDs) featuring a 10-15 nm bulk-size CdS core overcoated with a 4-5 nm CdSe shell (Fig. 5b-5e).[91] Similar to other quantum well colloids, the nanoshell architecture offers a larger volume of the carrier confinement as compared to zero- or one-dimensional nanocrystals, which is expected to reduce the rate of the multiexciton Auger recombination.[90] Furthermore, owing to the two-dimensional geometry, semiconductor nanoshells are likely to display the continuous density of states[94,95] similarly to 2D nanoplatelets[96] and nanosheets colloids.[97] Consequently, the number of conduction states per nanoshell is no longer limited to two, as in the case of zero-dimensional CdSe, which should permit lasing without a complete occupation of the lowest-energy excitonic state.[98] One fascinating application of the nanoshell geometry lies in the combination of two- and zero-dimensional excitons within the same nanoparticle. An example of such nanocomposite, comprising a small PbS core, an intermediate shell of a wide-gap CdS, and a secondary shell of quantum-confined CdSe semiconductors, has been recently demonstrated by our group.[92] As illustrated in Fig. 5f, the PbS core can engage in the Förster resonant energy transfer with the CdSe shell causing the flow of excitations from the periphery to the center of the composite nano-object. The spatial separation between donor and acceptor domains in these materials is vital for suppressing their charge transfer interactions. Consequently, the reported PbS/CdS/CdSe core/shell/shell geometry can support an *intraparticle* energy

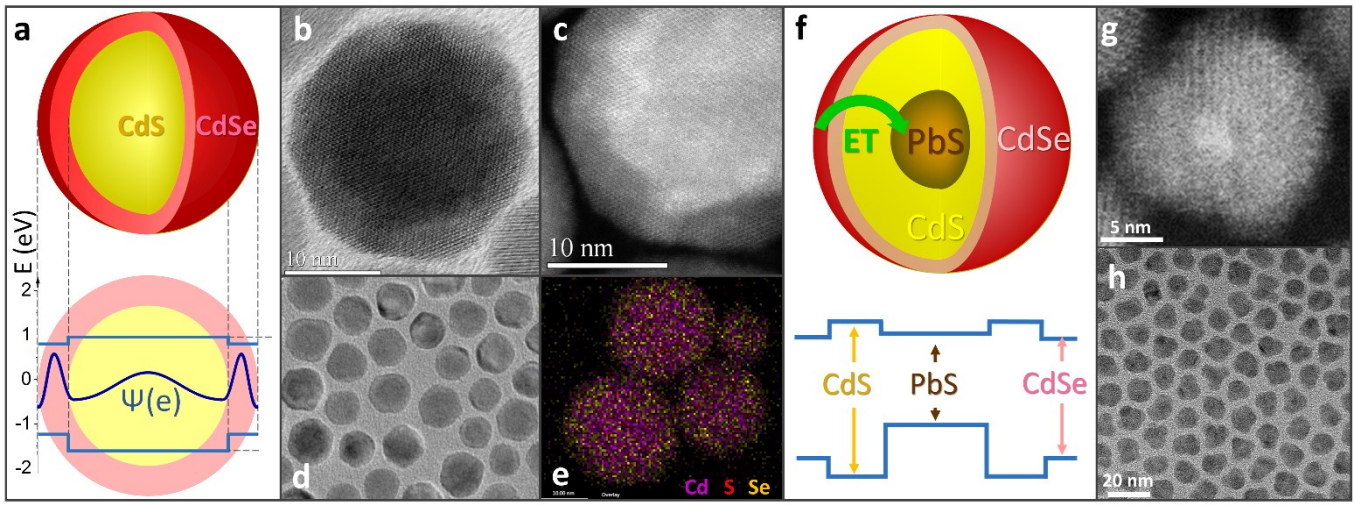

Figure 5. (a). Schematic illustration of the CdS/CdSe nanoshell geometry. The potential energy minima of the CdSe conduction and valence bands promote the shell-localization of both photoinduced charges. In this geometry, the core dimensions are allowed to exceed the exciton Bohr radius, leading to the quantum confinement in nanostructures approaching 30 nm in diameter. (b-e). High-resolution Transmission Electron Microscope (TEM) and high angle annular dark field (HAADF)-STEM images of CdS/CdSe nanoshell quantum dots. (f). Schematic representation of excited state energy levels in fabricated core/barrier/shell NCs. (g). Dark field STEM image of a PbS/CdS/CdSe nanocrystal indicating the presence of the PbS and CdSe domains through a color contrast. A somewhat darker shading around a bright center area is ascribed to be a CdS barrier. (h). Low-resolution TEM image of PbS/CdS/CdSe NCs. Figures adapted with permissions from ref. 91 and 92. Copyright 2017 American Chemical Society.

transfer, a phenomenon, which has also been demonstrated using several other semiconductor architectures. [99-101]

Metal-semiconductor energy transfer in plasmonic assemblies.

The transfer of the localized energy between semiconductor nanocrystals and metal nanoparticles represents another popular mechanism of the photoinduced energy conversion. The plasmon-exciton energy exchange has long been investigated towards enhancing the light absorption in photovoltaic devices as well as for modulating the emission of proximal dyes in biosensing applications. In the weak coupling regime, metal and semiconductor components exhibit a low overlap of electronic wave functions allowing energy transfer processes to undergo primarily *via* dipole-dipole interactions.[102] Early studies focusing on metal-enhanced absorption and fluorescence in semiconductors[103-112] outlined basic mechanisms of such energy exchange, concluding that plasmon-exciton interactions in these systems can enable both forward (PIRET) and backward (FRET) directions of the energy flow (Fig. 6c). Such bilateral energy exchange is responsible for a frequently observed competition between the plasmon-induced enhancement and quenching of semiconductor excitations, (ΔN_{PIRET})>1 and (ΔN_{FRET} <1), respectively. Overall, the net gain in the exciton population of the semiconductor nanocrystal due to a proximal plasmon can be expressed as:

$$\Delta N = \Delta N_{PIRET} \times \Delta N_{FRET} = \left(1 + E_{PIRET}\right) \times \left(1 - E_{FRET}\right) =$$
$$= \left(1 + \frac{\alpha_{plasmon}}{\alpha_{semi}} \times \frac{1}{1 + \left(R/R_0^{PIRET}\right)^n}\right) \times \left(1 - \frac{1}{1 + \left(R/R_0^{FRET}\right)^n}\right) \quad (1)$$

where n = 4-6 depending on whether the dipoles are considered to be surface- or point-like, α represents the wavelength-dependent absorbance coefficient, and R_0 is the donor-acceptor distance corresponding to a 50% efficiency. This equation does not take into account the photoinduced charge transfer between metal and semiconductor moieties, which reduces the exciton population of the latter.

Plasmon-enhanced fluorescence (FL) represents one of most studied realizations of the metal-semiconductor energy transfer. Generally speaking, the FL of a semiconductor can be either enhanced by a proximal metal surface through a plasmon induced resonant energy transfer (PIRET) or quenched *via* the exciton-to-plasmon ET (*via* FRET). Many of the literature reports on plasmon-enhanced FL have actually demonstrated quenching of the emission, $\Delta FL_{plasmon} < 1$, particularly when the size of a metal nanoparticle falls below 20 nm.[113-117] In this size regime, quenching *via* FRET (Eq. 1), as well as the photoinduced charge transfer back to the metal overwhelm the effect of PIRET-based enhancement.[118] Experimental observations of the plasmon-enhanced fluorescence ($\Delta FL_{plasmon} > 1$) have been almost exclusively limited to systems featuring large-diameter metal nanoparticles often exceeding 30 nm in size.[119-124] The corresponding FL enhancement factors appeared to be particularly large in the case of metal nanorods, where slower dephasing surface plasmons[125-127] exhibited a greater probability of interacting with semiconductor excitons through the PIRET mechanism. In the case of weakly emitting dyes, the PL gain is further increased by the plasmon-enhancement of the semiconductor radiative rates.

The prospect of employing the plasmon-exciton energy transfer in photovoltaic devices has received an increased

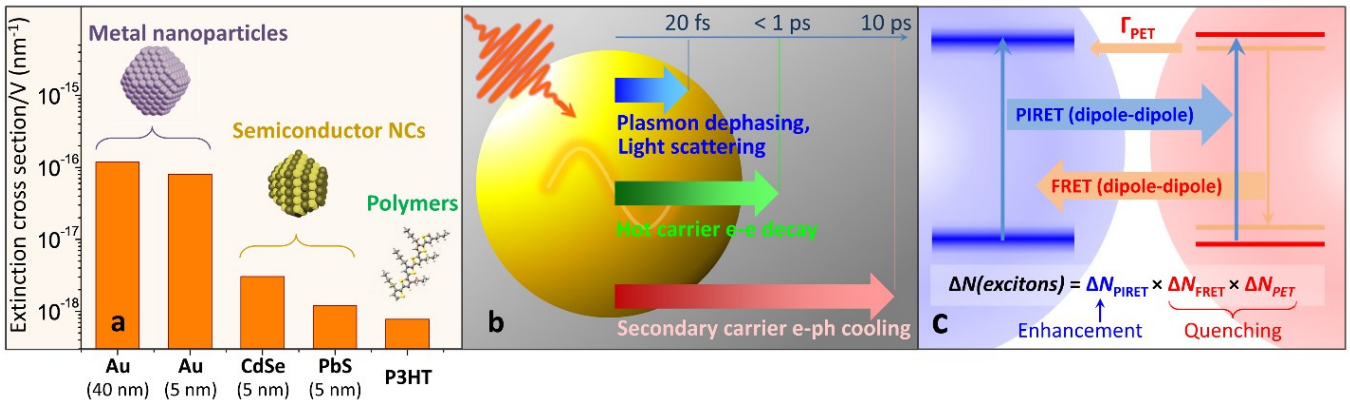

Figure 6. Plasmon-exciton energy exchange. (a). Extinction cross sections of common nanoscale sensitizers divided by the nanoparticle volume. The comparison highlights superior light-harvesting characteristics of metal nanoparticles in comparison to semiconductor quantum dots and organic polymers (e.g. P3HT). Adapted with permission from Ref.24. Copyright 2014 American Chemical Society. (b). The time scale of the surface plasmon evolution in noble metal nanoparticles, including stages of plasmon dephasing (10-20 fs), hot carrier redistribution (200 fs – 1 ps) *via* electron-electron decay, and electron-phonon cooling (1 -10 ps). (c). A diagram illustrating possible FL enhancement and quenching mechanisms in a metal-semiconductor system. The near-field energy exchange between electrical dipoles of the plasmon and semiconductor permits both forward (PIRET) and backwards (FRET) direction of the energy transfer. Photoinduced electron transfer (PET) can also contribute to quenching of the semiconductor emission.

amount of attention in recent years.[24,128-137] The expected benefits of incorporating plasmonic materials within solar cells stem from a large optical extinction of metal nanoparticles, which exceeds that of similar size semiconductors by 2 orders of magnitude (Fig. 6a). Consequently, the plasmon-enhanced absorption represents a potentially feasible strategy for improving the performance of solar cells. In this regard, the resonant transfer of plasmon energy offers the potential for a higher gain in the photoinduced carrier generation than the threshold-limited process of plasmon-induced hot electron transfer.[138-142] The expectations are supported by theoretical estimates of the relative plasmon enhancement in Fig. 7a, which compares the relative enhancement factors from far-field (scatter), near-field (PIRET), and hot electron based plasmon energy conversion.

The effect of the PIRET process on the power conversion efficiency (PCE) of photovoltaic devices has been investigated in our earlier work on quantum dot solar cells.[24] The absorber layer consisted of PbS NC solids blended with spherical Au nanoparticles as shown in Fig. 7d. In this geometry, far field scattering of surface plasmons was suppressed due to the relatively small size of Au nanostructures (< 10 nm). The thermal impact of plasmon excitations was mitigated through the use of an all-inorganic film design featuring a crystalline matrix encapsulating array of Au and PbS nanoparticles.[33,34,46] The overall benefit of the near-field absorption enhancement strategy was evidenced through a moderate improvement of the solar cell efficiency (Fig. 7c). For instance, the incorporation of 0.3% of Au NPs (by particle volume) has enhanced the average power conversion efficiency (PCE) from 4.0 to 4.2%, with the best performing device exhibiting 4.5% of PCE (Fig. 7c). The increased short circuit current (a gain of 41 ± 3%) was the primary factor contributing to the enhanced PCE, whose effect was somewhat reduced owing to a small drop in the open circuit voltage.

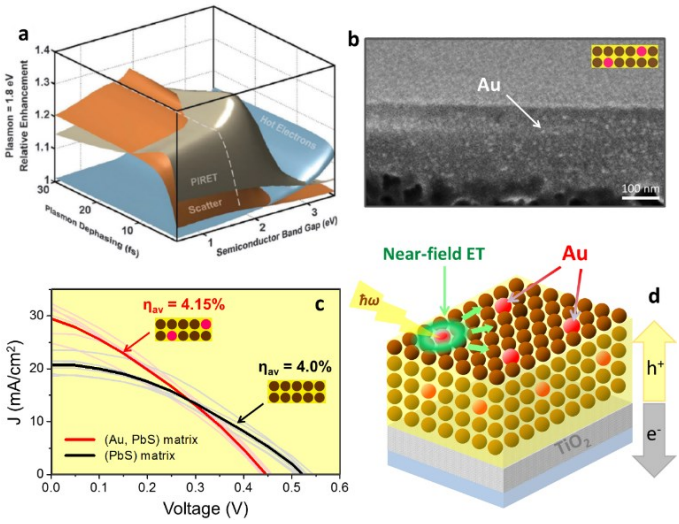

Figure 7. (a). Theoretical estimates of the relative plasmon enhancement corresponding to far-field (scattering), near-field (PIRET), and hot electron based plasmon energy conversion processes *versus* the plasmon's dephasing stage and the semiconductor band gap (the plasmon energy fixed at 1.8 eV). Adapted from Ref.143 with permission from the PCCP Owner Societies. (b). Scanning Electron Microscope image of a plasmonic solar cell absorber comprising a matrix-encapsulated (PbS, Au) film. (c). Current-voltage characteristics of plasmonic (Au, PbS) and control (PbS-only) quantum dot solar cells. The relatively low photovoltage of plasmonic solar cells was believed to be caused by Au-induced Fermi level pinning (d). Schematics of the depleted heterojunction PV cell doped with Au nanoparticles. Adapted with permission from Ref.24. Copyright 2014 American Chemical Society.

Dye-semiconductor energy-transfer system

The near-field energy exchange between semiconductor nanocrystals and dye molecules represents another prevalent mechanism of the photoinduced energy conversion. Historically, early applications of this process have involved dye-sensitized assemblies of quantum-confined semiconductors and oxides.[144-148] These materials were developed primarily as electrodes for photocatalytic or photovoltaic applications as detailed by several relevant reviews on the subject.[149-153] Besides the photoinduced energy conversion, the near field interaction of semiconductor nanocrystals and dye molecules has been employed for sensing biological processes in tissues and live cells.[7,154-157] This approach relied on detecting distance-dependent changes in the semiconductor-dye FRET efficiency as a strategy for measuring the concentration of a particular analyte that docks at a known distance to a host,[158] or for determining the spatial separation between fluorescent labels in targeted macromolecules.[159-

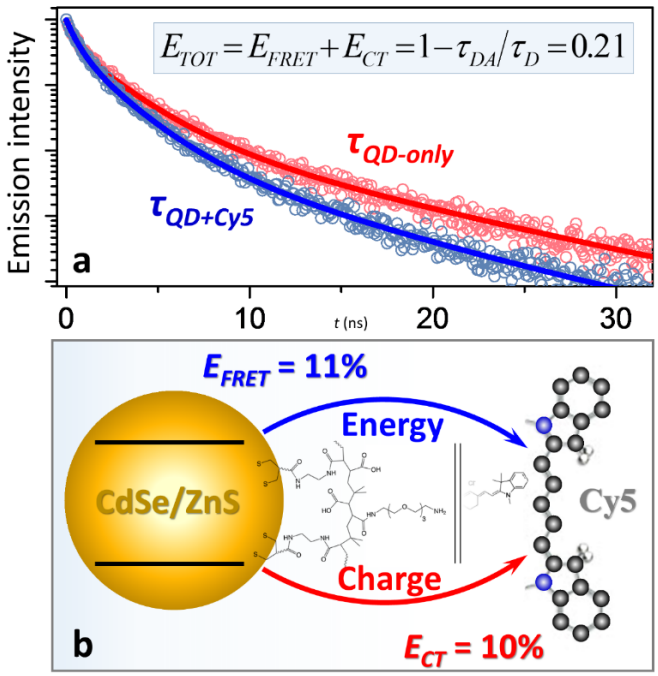

Figure 8. Donor-acceptor assemblies of CdSe/ZnS semiconductor nanocrystals and cyanine dyes (Cy5) exhibiting an interplay of charge and energy transfer processes. (a). The PL lifetimes of donor-only (CdSe/ZnS NCs) and donor-acceptor (CdSe/ZnS-Cy5) samples were used to calculate the total donor PL quenching efficiency, E_{tot} = 21%. (b). Partial contributions from energy (E_{ET} = 11%) and charge (E_{CT} = 10%) transfer processes were determined using the STEP spectroscopy.

The utilization of semiconductor nanocrystals as FRET donors has been steadily advanced over the years. Some remaining issues concern the explicit location of the nanocrystal's dipole and its orientation compared to molecular fluorophores. In addition, any potential contribution of charge transfer (CT) processes to donor PL quenching represents a potential source of error, which inflates the measured FRET efficiency. Such CT processes were shown to be considerable in the case of dye-nanocrystal assemblies comprising ruthenium complexes,[163] metal ions or organic conductors.[164-166] In order to distinguish between charge transfer and energy transfer processes in donor-acceptor assemblies, our group has developed the Sample Transmitted Excitation Photoluminescence (STEP) spectroscopy approach[167] that correlates the loss of donor excitons with the gain in the acceptor emission. By applying this technique to biosensor assemblies of cyanine dyes (Cy5, Cy7) and CdSe/ZnS nanocrystals, we were able to determine that the charge transfer accounts for 50-99% of donor emission quenching (see Fig. 8). For instance, for a QD-Cy5 system, exhibiting a significant donor-acceptor spectral overlap, approximately half of the total quenching efficiency, E_{tot} = 0.21 (Fig. 8a), was due to FRET (Fig. 8b) with the other half originating from other acceptor induced processes, such as the QD→Cy5 charge transfer. Meanwhile, in the case of a low-overlap QD-Cy7 construct (where ET is mostly suppressed), the observed 50-60% reduction in the donor PL lifetime (E_{tot} = 0.5-0.6) was almost entirely attributed to non-FRET processes. This result demonstrates the importance of determining CT efficiencies in a spectroscopic ruler and other FRET-based sensing applications.

The transfer of singlet excitons represents the most studied mechanism of energy diffusion in nanocrystal assemblies. A number of recent works, however, have demonstrated the possibility of triplet energy exchange between semiconductor nanocrystals and organic molecules.[168-173] This process was originally observed to proceed from organic semiconductors (tetracene, pentacene) to lead chalcogenide nanocrystals[168,169] and was later demonstrated to progress in the opposite direction, in which case triplet excitons of CdSe and PbS nanocrystals were transferred to organic acceptors, such as surface-anchored polyaromatic carboxylic acid or rubrene films (see Fig. 9).[173-177]

The successful transfer of triplet excitons from semiconductor nanoparticles to bulk solutions implies a general scheme by which quantum-confined colloids can be utilized as effective surrogates for molecular triplets. Semiconductor nanoparticles could thereby sensitize a variety of chemical reactions relevant to fields of optoelectronics, solar energy conversion, and photobiology. One attractive possibility is this regard pertains to employing semiconductor nanocrystals as triplet sensitizers of photoredox coordination compounds. Coupling of nanocrystal sensitizers to organometallic catalysts can allow avoiding the energy losses associated with intersystem crossing to a triplet state since the singlet-triplet splitting in nanocrystals is minimal.[171,178,179]

Experimental strategies for measuring the energy transfer in nanocrystal systems

Experimental measurements of the exciton diffusion in nanocrystals are complicated by the fact that no net charge is being transferred between photoexcited species. In this regard,

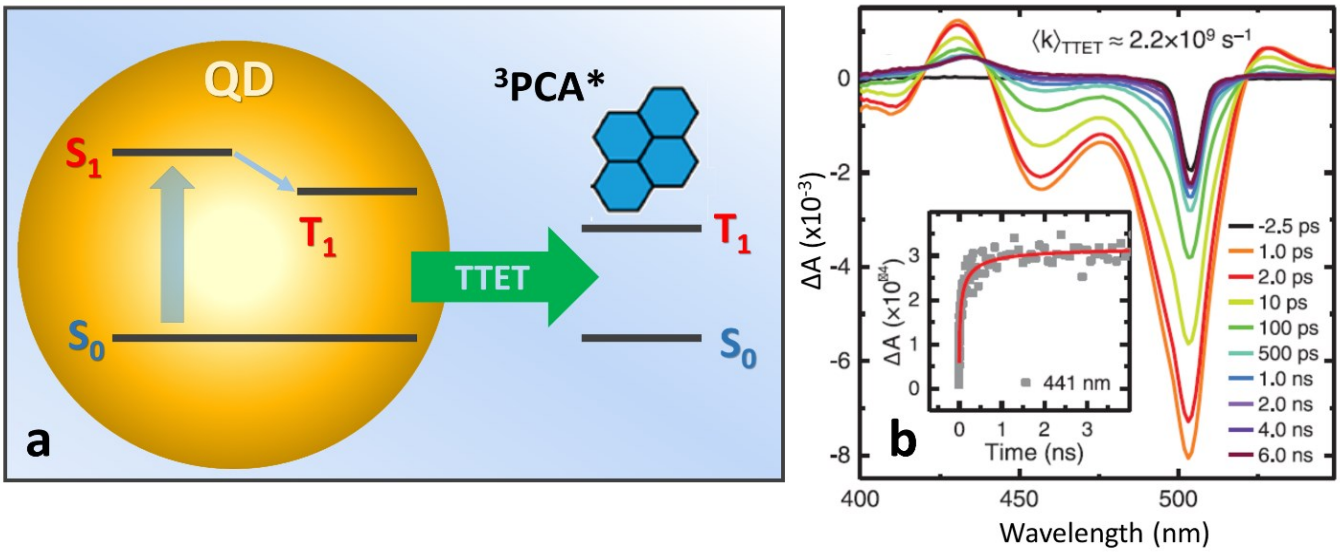

Figure 9. (a). Illustration of the triplet energy transfer between a nanocrystal donor and a triplet acceptor (PCA). (d). Ultrafast transient absorption spectra of CdSe-OA nanocrystals in toluene solution upon selective excitation of CdSe, using 500-nm pulsed laser excitation in the presence of surface-anchored 9-anthracenecarboxylic acid ACA in toluene. The inset in (d) shows TA kinetics monitored for the growth of ^{3}ACA at 441 nm. Reproduced with permission from Ref. 170. Copyright 2016 AAAS.

optical techniques provide an almost exclusive probe of the energy flow across excitonic materials.[2,54,55,180] When the nanocrystal energy is shared with molecular dyes, many aspects of the ET dynamics could be obtained from the acceptor-induced quenching of the donor emission. If τ_{DA} and τ_D are the donor PL lifetimes in the presence and absence of an acceptor, respectively, the energy transfer efficiency, *E*, and the corresponding ET rate, Γ, are given by:

$$E = 1 - \tau_{DA}/\tau_D \text{ and } \Gamma = 1/\tau_{DA} - 1/\tau_D \qquad (2)$$

These equations are accurate as long as the energy transfer represents the primary mechanism of the donor emission quenching (negligible charge transfer contribution).

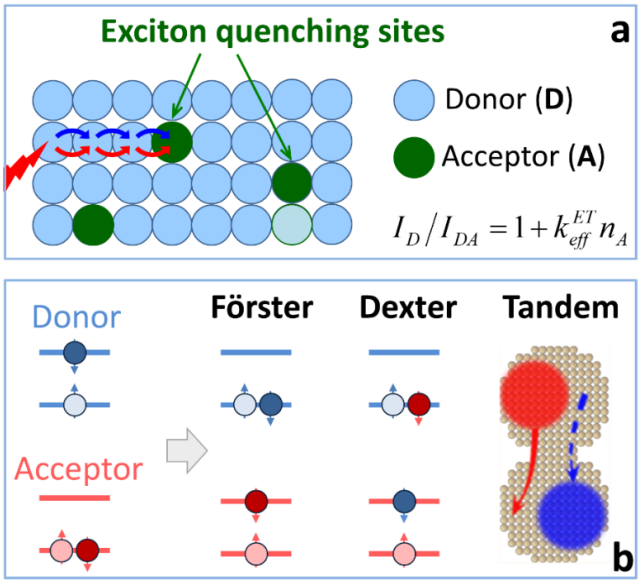

Figure 10. (a). Bulk quenching approach for measuring the energy transfer dynamics in nanocrystal solids. The technique relies on doping the investigated film with randomly distributed acceptors (A). The resulting reduction in the emission of a blended solid due to exciton quenching by acceptor dots, I_D/I_{AD}, is proportional to the concentration of the acceptor *A*, as expressed by the equation in the insert. A linear fit to this equation can then be used to extract the rate of interparticle energy transfer, Γ_{ET} (*D*→*A*). Reproduced with permission from Ref. 180. Copyright 2017 American Chemical Society. (b). Illustration of the known mechanisms of energy transfer in nanocrystals solids, including Förster, Dexter, and tandem ET processes. The portion of the image is reproduced with permission from Ref. 181. Copyright 2016 American Chemical Society.

Similar strategies are used for measurements of the energy transfer across nanocrystal assemblies. In this case, the majority of experimental techniques built upon the concept of funneling exciton energy to low-energy "acceptors" strategically positioned across the sample.[182] Their temporal and spatial resolution has been recently enhanced with new imaging capabilities utilizing time-resolved optical microscopy,[183] transient absorption,[184-187] and transient photoluminescence quenching.[188] Lastly, the STEP spectroscopy has been introduced as a strategy that distinguishes between energy and charge transfer processes in nanocrystal solids.[167]

Bulk quenching represents one of the early spectroscopic strategies for probing the intermolecular energy transfer in nanoparticle solids. It was first introduced for energy transfer measurements in molecular solids[182] and subsequently adapted by Kagan[189] and Klimov[190] groups for measuring the exciton diffusion rates in nanocrystal films. Overall, the concept of the

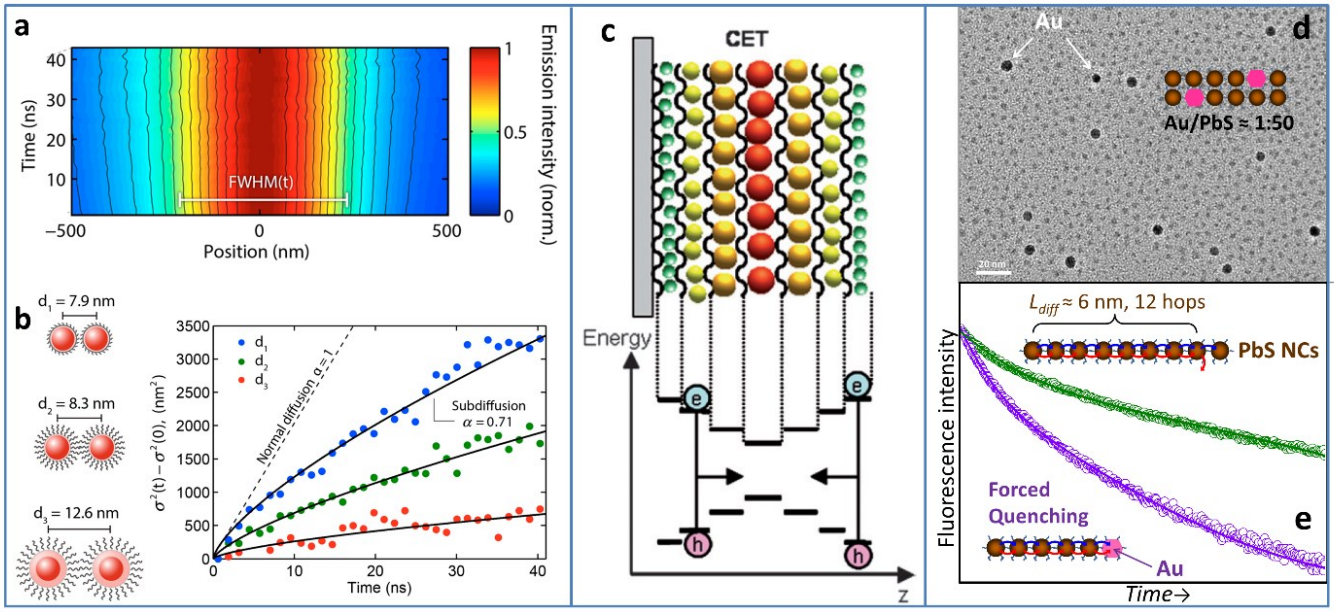

Figure 11. (a). Experimental time-evolution of the PL spatial cross-section for CdSe/CdS solids. The linear color scale indicates normalized PL intensity. (b) Schematic representation of the three types of quantum dot samples studied. The right panel shows the change in variance, σ^2, of the exciton distribution as a function of time for the three samples. The dashed line represents the hypothetical case of normal diffusion in which the variance grows linearly with time. Reproduced with permission from Ref.197. Copyright 2014 American Chemical Society. (c). Cascaded energy transfer sample (CET) consists of subsequent layers comprising green, yellow, orange, red, orange, yellow, and green emitting NCs. Below the CET sample the HOMO and LUMO are sketched, visualizing the cascaded band gaps used to facilitate cascaded energy transfer. Reproduced with permission from Ref.69. Copyright 2004 American Chemical Society. (d). TEM image of a mixed (Au + PbS) nanoparticle sample representing donor (PbS) – acceptor (Au) blend. (e). Schematic illustration of PL lifetime changes in blended films of Au and PbS NCs. By correlating PL changes with a concentration of quenching nanoparticles (Au), we have determined the average number of exciton hops and the corresponding exciton diffusion length. Reproduced with permission from Ref.61. Copyright 2015 American Chemical Society.

bulk quenching is based on blending the investigated solid of nanoparticles *D* with randomly distributed "acceptor" nanoparticles *A* (Fig. 10a), which trap excitons in potential energy minima. Excitons funneled into acceptor sites may recombine radiatively (bulk activation) or quenched through non-radiative channels (bulk quenching). In both cases, the diffusion length of excitons in a blended solid is restricted to a smaller volume due to the presence of quenching sites. As a result, the lifetime of donor excitons in a blended solid becomes reduced due to a shorter travel, causing the donor PL intensity as well as its lifetime to diminish. If the concentration of quenching nanoparticles is small, $n_A \ll n_D$, the ratio of the emission intensity in a pure sample (D) to that of an acceptor-doped film (DA) is expressed linearly with the quencher concentration, n_A: $I_D/I_{DA} = 1 + K_{eff} n_A$, where I_D is the PL intensity of a pure QD solid, I_{DA} is the emission intensity of a doped film, and k_{eff} is an effective energy transfer parameter. The application of the bulk quenching strategy to NC solids usually relies on doping nanocrystal solids with larger nanoparticles of the same semiconductor material[55,189,191] or by introducing ''energy gradient'' bilayer structures (Fig. 11c).[69,190,192]

The spatial extent of the exciton diffusion in nanocrystal solids can be characterized by introducing emission-quenching sites in *lieu* of fluorescent acceptors (*A*). This strategy was demonstrated in our recent study,[61] where "PL quenching" Au nanoparticles were introduced into investigated solids of PbS nanocrystals (Fig. 11d). By correlating the Au-Au interparticle distance in the film with corresponding changes in the PbS emission lifetime (Fig. 11e), it was possible to obtain important transport characteristics, including the exciton diffusion length, the number of pre-dissociation hops, the rate of interparticle energy transfer, and the exciton diffusivity. In particular, we found that for MPA-linked solids (interparticle distance = 0.9 nm), excitons diffused to an average length of 5.7 nm in approximately 12 hops, which corresponded to the diffusivity of 0.012 cm^2s^{-1}. Meanwhile, MOA-linked solids (interparticle distance = 1.7 nm) gave rise to a longer diffusion length of 11.4 nm (34 hops) and a lower diffusivity of 0.003 cm^2s^{-1}. The observed difference in the dynamics of the two film types was explained as due to the charge-tunneling mechanism of the exciton dissociation.

In addition to bulk quenching, other methodologies based on temperature-resolved PL[193-196] and optical microscopy[183,197] have been developed for probing the exciton dynamics in nanocrystal films. For instance, Bulović and Tisdale have reported direct visualization of the exciton transport in nanocrystal assemblies by using time-resolved fluorescence microscopy.[183,197] The demonstrated method was used to obtain a diffraction-limited profile of the energy flow across the

solid, which was recorded in a time-dependent manner (Fig. 11a). By supporting the spatial imaging data with kinetic Monte Carlo simulations, the study revealed that the energy disorder of nanocrystal solids resulted in a time-dependent diffusivity, with diffusion proceeding more slowly as excitons move energetically downhill (Fig. 11b).

FRET represents the primary process of energy transfer in a variety of nanocrystal-based systems, including quantum dot solids, dye-nanocrystal conjugates, and metal-nanocrystal assemblies. Experimental measurements of the FRET efficiency in these systems are usually performed by analyzing the changes in the donor emission, according to Eq. 2.[198-200] The intrinsic error associated with such measurements comes from non-FRET contributions to donor emission changes that arise from the acceptor-induced dissociation of donor excitons, broadly defined as the charge transfer (CT).[201-204] Consequently, the measured total efficiency of the donor PL quenching, E_{TOT}, in general, may include contributions from both FRET and CT processes. This is particularly problematic for systems featuring a significant driving force for the photoinduced charge transfer, where the donor-acceptor distance can no longer be estimated by assuming FRET-only contribution.

STEP spectroscopy[167] was recently introduced as a viable strategy for distinguishing between the energy and charge transfer processes in donor-acceptor systems. This technique correlates the changes in the acceptor emission with the spectral modulation of the donor excitation spectrum, which allows extracting FRET-only efficiencies, independently of the charge transfer contribution. Moreover, by relying on the acceptor emission, the STEP spectroscopy becomes amenable for characterizing systems with non-emissive donor species (e.g. plasmonic nanoparticles).

The details of the STEP technique for measuring the energy transfer efficiency in donor-acceptor assemblies have been described in recent literature (see Refs. 167,205-207). The method is based on the assumption that the number of photons emitted by an acceptor fluorophore, N_A^{PL}, depends linearly on the number of excited acceptor (*A*) and donor (*D*) molecules, N_A and N_D, respectively:

$$N_A^{PL} = QY_A(N_A + E_{D\to A}N_D) \quad (3)$$

where $E_{D\to A}$ is the quantum efficiency for the *D*→*A* energy transfer, and QY_A is the emission quantum yield of the fluorophore *A* in the presence of the fluorophore *D* (as measured in the donor-acceptor assembly). To determine $E_{D\to A}$, a donor-acceptor sample is excited using a broad-band light source and the emission intensity of the acceptor dye, $N_A^{PL}(E)$, is recorded. The excitation light is then spectrally shaped using donor-like or acceptor-like filters (Fig. 12a) designed to suppress the excitation of donor or acceptor species in the investigated sample (N_D << N_A or N_A << N_D, respectively). If the spectral profile of the excitation light, $n(\lambda)$, and the optical density (OD) of the excitation filter are known, one can predict the change in the acceptor emission as a function of a single parameter, $E_{D\to A}$. Figures 12b,c illustrate the procedure for extracting the energy transfer efficiencies from STEP measurements utilizing two types of excitation filters. In Fig. 12c, this strategy is described for a donor-type excitation filter (e.g. a solution of donor molecules), which spectral profile is suitable for suppressing the excitation of donor molecules in the sample, causing the acceptor emission to change proportionally to $E_{D\to A}$. These changes are best illustrated by plotting a normalized acceptor emission, $f_D = N_A^{PL}/N_A$, as a function of the donor-type filter optical density. The measured parameters, M_1 and M_2, are then used to calculate the energy transfer efficiency, as follows:

$$E_{D\to A} = (M_1/M_2) \times (N_A^0/N_D^0) \quad (4)$$

where (N_A^0/N_D^0) represents the ratio of acceptor to donor excitations in the sample prior to the application of the excitation filter, determined from relative amplitudes of excitation and absorption profiles. Alternatively, one can fit the experimental f_D with a model parametric curve, f_{theor}, featuring a single fitting parameter, $E_{D\to A}$. To obtain $f_{theor}(E) = N_A^{PL}(E)/N_A$, $N_A^{PL}(E)$ is determined using Eq. 3 as a parametric function of the energy transfer efficiency, *E*. The value of N_A is calculated according to Ref. 167. When the acceptor-like excitation filter is used (e.g. a solution of acceptor molecules), the energy transfer efficiency, $E_{D\to A}$, is obtained from the acceptor emission scaled by the number of donor excitations, $f_D = N_A^{PL}/N_D$. Figure 12b shows the projected evolution of f_A with the increasing optical density of the acceptor-type excitation filter. The experimental parameters, M_1 and M_2, can then be used to determine $E_{D\to A}$ either directly from the equation in Fig. 12b or by fitting the experimental f_A with a model parametric curve, $f_{theor}(E_{D\to A})$.

The ability of the STEP approach to distinguish between charge and energy transfer processes has been demonstrated using several donor-acceptor systems. One of these works have utilized a simplified system of nanocrystal solids comprising an assembly of small (*d* = 3.5 nm) and large (*d* = 4.5 nm) core CdSe/CdS NCs (Fig. 12d).[167] Prior investigations of similar assemblies by means of the bulk quenching approach have concluded that the energy transfer between proximal CdSe/CdS dots competes with the process of the interparticle charge transfer, which causes the dissociation of excitons. The corresponding dissociation probability was estimated to be p_{diss} ≈ 6% for assemblies featuring oxalic acid linkers.[68] STEP measurements of similarly prepared solids have confirmed this premise. It was estimated that ≈ 30% of excitons in donor species (smaller-diameter CdSe/CdS) were transferred to larger-diameter nanocrystals, meanwhile, ≈ 2% of excitations were dissociated due to the charge transfer involving acceptor dots. In another experiment, the STEP spectroscopy was used to unravel the interplay of charge and energy transfer processes in assemblies of CdSe/ZnS nanocrystals and cyanine dyes (Fig. 12e). By using a combination of STEP and donor PL quenching measurements, we observed that in the case of a QD-Cy5 system, exhibiting a significant donor-acceptor spectral overlap, up to 50% of donor emission was quenched due to non-FRET processes. Finally, the STEP spectroscopy was applied for estimating the quantum efficiency of the photoinduced energy

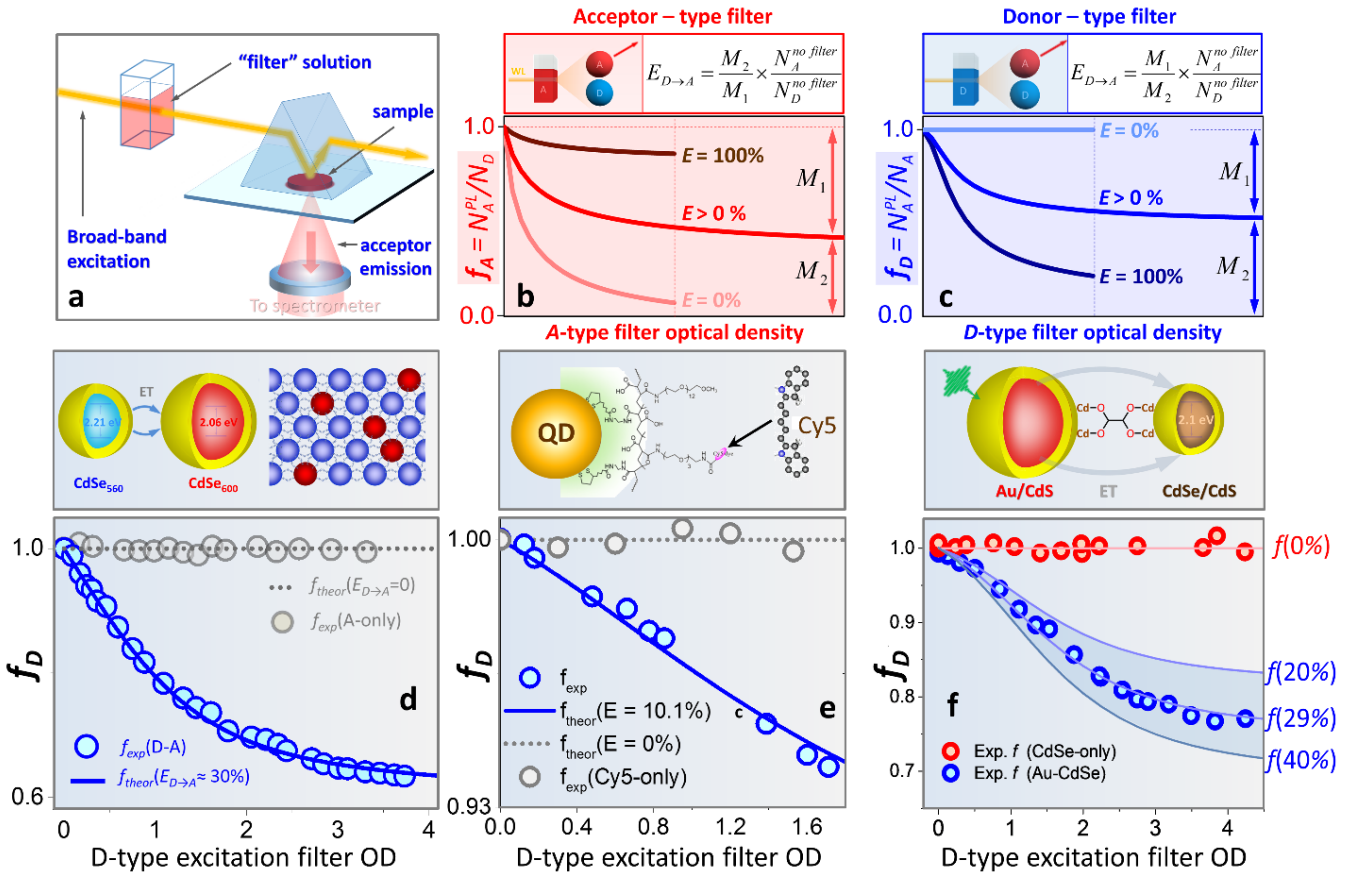

Figure 12. (a). An illustration of the STEP spectroscopy setup. (b). STEP measurements utilizing an acceptor-type excitation filter. The energy transfer efficiency, $E_{D\to A}$, is obtained from the acceptor emission by using experimental parameters, M_1 and M_2 (see insert). Alternatively, one can fit the experimental data points, f_A, with a model parametric curve, $f_{theor}(E_{D\to A})$, featuring a single fitting parameter, $E_{D\to A}$. (c). STEP measurements utilizing a donor-type filter that preferentially suppresses the excitation of donor molecules in the sample causing the acceptor emission to change proportionally to $E_{D\to A}$ (see insert). (d). STEP measurements of donor ($CdSe_{560}$)-acceptor ($CdSe_{600}$) nanocrystal assemblies. The f_{exp} ratio measured *versus* the *D*-filter optical density (OD) for acceptor-only (grey circles) and donor-acceptor (blue circles) solids. Experimental data is fitted with a parametric model curve, $f_{theor}(E_{D\to A})$, resulting in $E_{D\to A}$ = 30%. (e). CdSe/ZnS-Cy5 assemblies. The evolution of the scaled acceptor (Cy5) emission $f_D = N_A^{PL}/N_D$ *versus* the optical density of the donor-type excitation filter (Cy3). The experimental data is best fitted with a f_{theor}(*E* = 10.1%) model curve. f_D measured for the acceptor-only control sample (Cy5 solution) reveals no dependence on the donor-filter optical density (gray dots), consistent with the absence of ET in this case. (f). STEP measurements of the metal-to-semiconductor ET in assemblies of 21-nm Au and CdSe/CdS NCs. Evolution of the scaled NC emission (*f*-ratio) *versus* the optical density of the donor-type excitation filter (Cy3.5) is shown by blue circles. The experimental data for Au-CdSe assemblies was fitted with a set of model parametric curves, indicating that $E_{Au\to CdSe}$ = 29-30%. *f*-ratio measured for the acceptor-only control sample (CdSe NC film – red circles) is independent of the donor-filter optical density.

transfer from plasmon resonances of metal nanoparticles to semiconductor nanocrystal matrices in assemblies of Au nanoparticles and CdSe nanocrystals, which represent a suitable model system of plasmonic antennas. We showed that in the case of 9.1-nm Au nanoparticles, only 1-2% of the Au absorbed radiation was converted to excitons in the surrounding CdSe nanocrystal matrix. For larger, 21.0-nm Au, the percentage of absorbed photons that was converted to excitons in CdSe NCs increased to 29.5% (Fig. 12f).[205]

Summary and Outlook

Size-dependent properties of semiconductor nanocrystals offer exciting opportunities for controlling the energy transfer dynamics on nanoscale. Thus far, the employment of band gap engineering appears to be the most prominent in the development of nanocrystal-dye biosensors and light-emitting materials. Going beyond these applications, the possibility of manipulating the energy transfer in nanocrystal assemblies is becoming increasingly attractive in areas of photocatalysis and photovoltaics. Some of the emerging trends in this regard are discussed below.

The realization of triplet states in semiconductor nanocrystals[170] can potentially enable light sensitization of photoinduced redox reactions. By engaging in the triplet energy transfer with molecular photoredox catalysts, such as $[Ru(bpy)_3]^{2+}$ or $Ir(ppy)_3$ coordination compounds,[208] nanocrystal

energy could be transformed into a long-lived triplet state (see Fig. 13a). Such energy conversion could be fairly fast, considering that the efficiency of triplet exciton transfer from CdSe to organic acceptors, such as ACA is greater than 90%.[170] Metal polypyridyl complexes represent particularly promising catalysts in this regard (Fig. 13a). Namely, photoexcited $[Ru(bpy)_3]^{3+}$ can oxidize water into O_2 and protons *via* a metal oxide catalyst (Fig. 13a),[209] while, $[Ru(bpy)_3]^{2+*}$ triplet states can be utilized for reducing methylviologen (*via* ligands), a recyclable carrier of electrons.

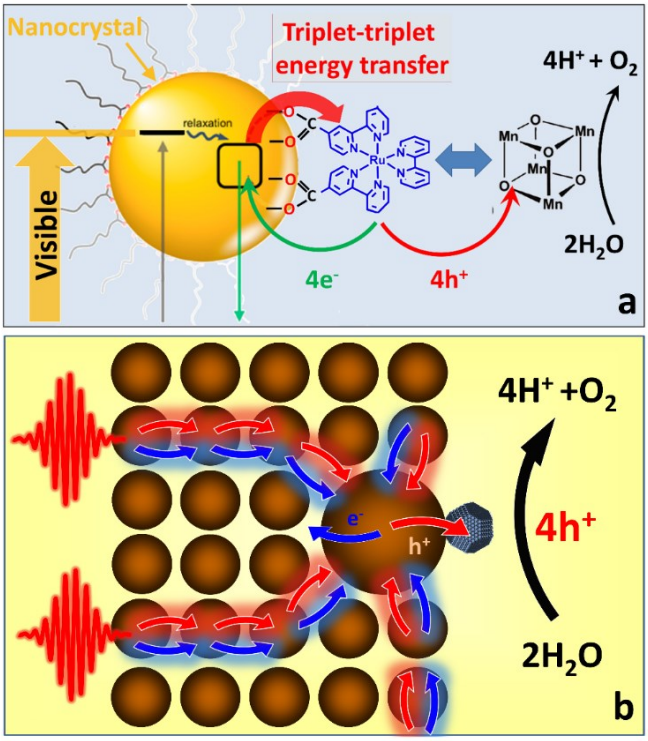

Figure 13. (a). A possible scheme for employing semiconductor nanocrystals as triplet sensitizers of organometallic catalysts. In this example, the triplet-triplet energy transfer from semiconductor nanocrystals to catalytically active ^{3}MLCT states of $[Ru(bpy)_3]^{3+}$ is utilized for water oxidation. (b). A possible strategy for concentrating the photoinduced energy in assemblies of semiconductor nanocrystals *via* the diffusion towards the low-energy reaction center. This scheme can potentially benefit multi-electron catalytic processes by increasing the probability of multiple charges to be collected on the same catalytic site. Reproduced from reference 210. Copyright 2018 Frontiers in Chemistry.

Employing semiconductor nanocrystals as triplet sensitizers of photoredox coordination compounds would allow avoiding many issues of nanocrystal photocatalytic systems related to photocorrosion, slow hole regeneration, and short excited-state lifetime. Furthermore, coupling nanocrystal sensitizers to organometallic catalysts will extend the usable portion of the solar spectrum. This is because the excitation of a triplet state in coordination compounds undergoes *via* a photon absorption into a singlet metal-ligand charge transfer state (^{1}MLCT) followed by a rapid intersystem crossing to a ^{3}MLCT state, which is commonly accompanied by an ~1 eV energy loss (due to large splitting of singlet and triplet states). Since such singlet-triplet splitting in semiconductor nanocrystals is usually much smaller (within thermal kT ~ 30 meV), the associated energy loss will be reduced. Another potential benefit is expected from the fact that the molar absorptivity of semiconductor nanocrystals, such as CdSe, is about 10-20 times greater[211] than that of the ^{1}MLCT transition in $[Ru(bpy)_3]^{2+}$ (~13 000 M^{-1} cm^{-1}in acetonitrile), which should result in the enhancement of the overall turnover frequency.

Like most excitonic systems, an assembly of semiconductor nanocrystals can allow energy concentration *via* the transfer of excitons from an excitation site to the acceptor domain associated with the potential energy minimum. Such energy-concentrating mechanism is utilized by biological systems, where multiple carriers are driven to the reaction center for catalyzing multi-electron processes. A demonstrative example of this process is the oxygenic photosynthesis in plants, where light is absorbed by hundreds of pigments (e.g chlorophylls) that transfer the photoinduced energy to a small number of special pigments (P680), capable of charge separation.[212] P680 will then share a photoinduced hole with a water-oxidizing complex (WOC).[213] After four oxidizing equivalents have been stored at the WOC site, it obtains four electrons from water molecules causing H_2O splitting. We expect that nanocrystal assemblies could be employed in a similar manner for driving multielectron catalytic processes, such as water oxidation or hydrogen production.[214,215] For instance, the diffusion of excitons in a nanocrystal solid to a nanoparticle with the smallest band gap[61,54,216] can be employed for collecting multiple excitons at the same site (Fig. 13b). The accepting dot could be appended with a catalyst to assist the charge separation. The presence of an electron- (or hole-) accepting catalysis would also allow avoiding the multiexciton populations on a single nanocrystal, which are subject to a rapid decay through the Auger recombination. Such nanocrystal assembly could be incorporated into a photoelectrochemical cell or harnessed within an "artificial leaf" platform.[217] Zero-dimensional nanocrystals in these assemblies could be substituted with either one- or two-dimensional nanostructures (e.g. nanosheets or nanoshell) in order to increase the energy transfer efficiency and reduce Auger recombination rates.

Plasmonics represents a fast developing area of nanoscience that exploits the ability of metal nanostructures to concentrate electromagnetic radiation. A related challenge concerns an efficient conversion of the plasmon-concentrated field into some form of useful energy. To address this issue, existing strategies based on the hot electron transfer and far-field scattering can be supplemented with a relatively novel scheme utilizing the plasmon induced resonant energy transfer (PIRET). The ultrafast nature of this process combined with the competition with the backward FRET calls for advanced imaging techniques. In this regard, near-field scanning optical microscopy (NSOM) offering deep subwavelength resolution appears to be particularly promising.[218,219] When equipped with time resolving capabilities[220], the ultrafast nanoscopy of

plasmonic structures can reveal the spatial dynamics of the evanescent field around metal nanostructures. The near-field scanning methods can be combined with the STEP spectroscopy for estimating the net energy flow in plasmon-semiconductor assemblies.

In collusion, colloidal semiconductor nanocrystals have emerged as a key material system for the development of nanoscale energy transfer platforms. The progress in this field is attributed to unique advantages of colloidal semiconductors that include tunable exciton energies and the ability to interface with a large variety of nanoscale energy-transfer partners, either through chemical conjugation or in solid assemblies. Thus far, most successful realizations of energy transfer reactions in nanocrystals involve single-step excitation transfers in molecular-nanoparticle assemblies. Nonetheless, the prospects of harvesting triplet excitons from nanocrystals or funneling the photoinduced energy in nanocrystal solids or plasmonic assemblies are rapidly gaining momentum. These energy-transfer systems hold strong promise for the development of new paradigms for solar energy production, solid state lighting, sensing, and near-field optical imaging applications.

Conflicts of interest

There are no conflicts to declare

Acknowledgements

This work was supported by the Award DE-SC0016872 (MZ) funded by the U.S. Department of Energy, Office of Science. PM was partly supported by NSF Award DMR-1710063. LRR was supported by NSF Award CHE-1465052.

Notes and references

[1] T. Ritz, A. Damjanović and K. Schulten, *ChemPhysChem,* 2002, **3**, 243-248
[2] P. Moroz, N. Kholmicheva, N. Razgoniaeva, D. Burchfield, N. Sharma, A. Acharya and M. Zamkov, *Chem. Phys.,* 2016, **471**, 59
[3] J. Lee, A. O. Govorov and N. A. Kotov, *Nano Lett.,* 2005, **5**, 2063.
[4] J. B. Hoffman, R. Alam and P. V. Kamat, *ACS Energy Lett.,* 2017, **2**, 391
[5] G. Pacchioni, *Nat. Rev. Mater.,* 2016, **1**, 16005.
[6] F. Piazza and Y. Sanejouand, *Phys. Biol.,* 2009, **6**, 046014
[7] K. D. G. Pfleger and K. A. Eidne, *Nat. Methods,* 2006, **3**, 165
[8] R. C. Somers, P. T. Snee, M. G. Bawendi and D. G. Nocera, *J. Photochem. Photobiol.*, 2012, **248**, 24
[9] A. L. Rogach, T. A. Klar, J. M. Lupton, A. Meijerink and J. Feldmann, *J. Mater. Chem.*, 2009, **19**, 1208
[10] R. C. Somers, M. G. Bawendi and D. G. Nocera, *Chem. Soc. Rev.,* 2007, **36**, 579
[11] C. S. Yun, A. Javier, T. Jennings, M. Fisher, S. Hira, S. Peterson, B. Hopkins, N. O. Reich and G. F. Strouse, *J. Am. Chem. Soc.,* 2005, **127**, 3115
[12] I. L. Medintz, A. R. Clapp, H. Mattoussi, E. R. Goldman, B. Fisher and J. M. Mauro, *Nat. Mater.,* 2003, **2**, 630.
[13] A. R. Clapp, I. L. Medintz, J. M. Mauro, B. R. Fisher, M. G. Bawendi and H. Mattoussi, *J. Am. Chem. Soc.,* 2004, **126**, 301
[14] I. L. Medintz, A. R. Clapp, F. M. Brunel, T. Tiefenbrunn, H. Tetsuo Uyeda, E. L. Chang, J. R. Deschamps, P. E. Dawson and H. Mattoussi, *Nat. Mater.,* 2006, **5**, 581
[15] E. Petryayeva, W. Russ Algar and I. L. Medintz, *Appl. Spectrosc.*, 2013, **67**, 215
[16] N. Hildebrandt, C. M. Spillmann, W. Russ Algar, T. Pons, M. H. Stewart, E. Oh, K. Susumu, S. A. Díaz, J. B. Delehanty and I. L. Medintz, *Chem. Rev.,* 2017, **117**, 536
[17] G. S. Engel, T. R. Calhoun, E. L. Read, T. K. Ahn, T. Mancal, Y. C. Cheng, R. E. Blankenship and G. R. Fleming, *Nature*, 2007, **446**, 782.
[18] C. E. Rowland, J. B. Delehanty, C. L. Dwyer and I. L. Medintz, *Mater. Today*, 2017, **20**, 131
[19] A. O. Govorov, G. W. Bryant, W. Zhang, T. Skeini, J. Lee, N. A. Kotov, J. M. Slocik and R. R. Naik, *Nano Lett.*, 2006, **6**, 984
[20] J. Lee, P. Hernandez, J. Lee, A. O. Govorov and N. A. Kotov, *Nat. Mater.*, 2007, **6**, 291
[21] L. Dyadyusha, H. Yin, S. Jaiswal, T. Brown, J. J. Baumberg, F. P. Booye and T. Melvin, *Chem. Commun.*, 2005, **0**, 3201
[22] F. Shaik, I. Peer, P. K. Jain and L. Amirav, *Nano Lett.*, 2018, **18**, 4370-4376
[23] Z. Liu, W. Hou, P. Pavaskar, M. Aykol and S. B. Cronin, *Nano Lett.,* 2011, **11**, 1111
[24] N. Kholmicheva, P. Moroz, U. Rijal, E. Bastola, P. Uprety, G. Liyanage, A. Razgoniaev, A. D. Ostrowski and M. Zamkov, *ACS Nano,* 2014, **8**, 12549
[25] M. Achermann, M. A. Petruska, S. Kos, D. L. Smith, D. D. Koleske and V. I. Klimov, *Nature*, 2004, **429**, 642
[26] C. Curutchet, A. Franceschetti, A. Zunger and G. D. Scholes, *J. Phys. Chem. C*, 2008, **112**, 13336
[27] Z. Chen, S. Berciaud, C. Nuckolls, T. F. Heinz and L. E. Brus, *ACS Nano*, 2010, **4**, 2964
[28] V. L. Colvin, M. C. Schlamp and A. P. Alivisatos, *Nature,* 1994, **370**, 354.

[29] S. Coe, W. Woo, M. Bawendi and V. Bulović, *Nature,* 2002, **420**, 800
[30] L. Sun, J. J. Choi, D. Stachnik, A. C. Bartnik, B. Hyun, G. G. Malliaras, T. Hanrath and F. W. Wise, *Nat. Nanotechnol.,* 2012, **7**, 369
[31] Y. Shirasaki, G. J. Supran, M. G. Bawendi and V. Bulović, *Nat. Photonics.,* 2013, **7**, 13.
[32] O. Chen, H. Wei, A. Maurice, M. Bawendi and P. Reiss, *MRS Bull.,* 2013, **38**, 696.
[33] P. Moroz, G. Liyanage, N. N. Kholmicheva, S. Yakunin, U. Rijal, P. Uprety, E. Bastola, B. Mellott, K. Subedi, L. Sun, M. V. Kovalenko and M. Zamkov, *Chem. Mater.,* 2014, **26**, 4256.
[34] E. Khon, S. Lambright, D. Khon, B. Smith, T. O'Connor, P. Moroz, M. Imboden, G. Diederich, C. Perez-Bolivar, P. Anzenbacher and M. Zamkov, *Adv. Funct. Mater.,* 2012, **22**, 3714.
[35] G. J. Supran, Y. Shirasaki, K. W. Song, J. Caruge, P. T. Kazlas, S. Coe-Sullivan, T. L. Andrew, M. G. Bawendi and V. Bulović, *MRS Bull.,* 2013, **38**, 703.
[36] G. J. Supran, K. W. Song, G. W. Hwang, R. E. Correa, J. Scherer, E. A. Dauler, Y. Shirasaki, M. G. Bawendi and V. Bulović, *Adv. Mater.,* 2015, **27**, 1437.
[37] M. Graetzel, R. A. J. Janssen, D. B. Mitzi and E. H. Sargent, *Nature,* 2012, **488**, 304.
[38] P. V. Kamat, *J. Phys. Chem. C,* 2008, **112**, 18737.
[39] I. Gur, N. A. Fromer, M. L. Geier and A. P. Alivisatos, *Science,* 2005, **310**, 462.
[40] O. E. Semonin, J. M. Luther, S. Choi, H. Chen, J. Gao, A. J. Nozik and M. C. Beard, *Science,* 2011, **334**, 1530.
[41] E. L. Rosen, A. M. Sawvel, D. J. Milliron and B. A. Helms, *Chem. Mater.,* 2014, **26**, 2214.
[42] G. H. Carey, A. L. Abdelhady, Z. Ning, S. M. Thon, O. M. Bakr and E. H. Sargent, *Chem. Rev.,* 2015, **115**, 12732.
[43] S. Keuleyan, E. Lhuillier, V. Brajuskovic and P. Guyot-Sionnest, *Nat. Photonics,* 2011, **5**, 489.
[44] G. Konstantatos, M. Badioli, L. Gaudreau, J. Osmond, M. Bernechea, Arquer, F. Pelayo Garcia de, F. Gatti and F. H. L. Koppens, *Nat. Nanotechnol.,* 2012, **7**, 363.
[45] G. Konstantatos, I. Howard, A. Fischer, S. Hoogland, J. Clifford, E. Klem, L. Levina and E. H. Sargent, *Nature,* 2006, **442**, 180.
[46] E. Kinder, P. Moroz, G. Diederich, A. Johnson, M. Kirsanova, A. Nemchinov, T. O'Connor, D. Roth and M. Zamkov, *J. Am. Chem. Soc.,* 2011, **133**, 20488.
[47] C. M. Chuang, P. R. Brown, V. Bulović and M. G. Bawendi, *Nat. Mater.,* 2014, **13**, 796.
[48] B. S. Mashford, M. Stevenson, Z. Popovic, C. Hamilton, Z. Zhou, C. Breen, J. Steckel, V. Bulovic, M. Bawendi, S. Coe-Sullivan and P. T. Kazlas, *Nat. Photonics,* 2013, **7**, 407.
[49] X. Lan, O. Voznyy, García de Arquer, F. Pelayo, M. Liu, J. Xu, A. H. Proppe, G. Walters, F. Fan, H. Tan, M. Liu, Z. Yang, S. Hoogland and E. H. Sargent, *Nano Lett.,* 2016, **16**, 4630.
[50] R. W. Meulenberg, J. R. I. Lee, A. Wolcott, J. Z. Zhang, L. J. Terminello and T. van Buuren, *ACS Nano,* 2009, **3**, 325
[51] J. J. Choi, J. Luria, B. Hyun, A. C. Bartnik, L. Sun, Y. Lim, J. A. Marohn, F. W. Wise and T. Hanrath, *Nano Lett.,* 2010, **10**, 1805.
[52] P. V. Kamat, *J. Phys. Chem. Lett.,* 2013, **4**, 908
[53] Y. Liu, M. Gibbs, J. Puthussery, S. Gaik, R. Ihly, H. W. Hillhouse and M. Law, *Nano Lett.,* 2010, **10**, 1960.
[54] D. Zhitomirsky, O. Voznyy, S. Hoogland and E. H. Sargent, *ACS Nano,* 2013, **7**, 5282.
[55] A. J. Mork, M. C. Weidman, F. Prins and W. A. Tisdale, *J. Phys. Chem. C,* 2014, **118**, 13920.
[56] M. Liu, O. Voznyy, R. Sabatini, Arquer, F. Pelayo García de, R. Munir, A. H. Balawi, X. Lan, F. Fan, G. Walters, A. R. Kirmani, S. Hoogland, F. Laquai, A. Amassian and E. H. Sargent, *Nat. Mater.,* 2017, **16**, 258
[57] P. Moroz, N. Kholmicheva, B. Mellott, G. Liyanage, U. Rijal, E. Bastola, K. Huband, E. Khon, K. McBride and M. Zamkov, *ACS Nano*, 2013, **7**, 6964
[58] Y. Liu, J. Tolentino, M. Gibbs, R. Ihly, C. L. Perkins,Y. Liu, N. Crawford, J. C. Hemminger and M. Law, *Nano Lett.*, 2013, **13**, 1578
[59] D. Zhitomirsky, O. Voznyy, L. Levina, S. Hoogland, K. W. Kemp, A. H. Ip, S. M. Thon and E. H. Sargent, *Nat. Comm.,* 2014, **5**, 3803
[60] Y. Cho, B. Hou, J. Lim, S. Lee, S. Pak, J. Hong, P. Giraud, A. R. Jang, Y.-W. Lee, J. Lee, J. E. Jang, H. J. Snaith, S. M. Morris, J. I. Sohn, S. N. Cha and J. M. Kim, *ACS Energy Lett.*, 2018, **4**, 1036
[61] N. Kholmicheva, P. Moroz, E. Bastola, N. Razgoniaeva, J. Bocanegra, M. Shaughnessy, Z. Porach, D. Khon and M. Zamkov, *ACS Nano,* 2015, **9**, 2926
[62] M. V. Kovalenko, R. D. Schaller, D. Jarzab, M. A. Loi and D. V. Talapin, *J. Am. Chem. Soc.,* 2012, **134**, 2457.
[63] M. V. Kovalenko, M. Scheele and D. V. Talapin, *Science,* 2009, **324**, 1417.
[64] D. V. Talapin, J. Lee, M. V. Kovalenko and E. V. Shevchenko, *Chem. Rev.,* 2010, **110**, 389.
[65] S. Yakunin, D. N. Dirin, L. Protesescu, M. Sytnyk, S. Tollabimazraehno, M. Humer, F. Hackl, T. Fromherz, M. I. Bodnarchuk, M. V. Kovalenko and W. Heiss, *ACS Nano*, 2014, **8**, 12883
[66] Z. Yang, O. Voznyy, G. Walters, J. Z. Fan, M. Liu, S. Kinge, S. Hoogland and E. H. Sargent, *ACS Photonics,* 2017, **4**, 830
[67] G. Diederich, T. O'Connor, P. Moroz, E. Kinder, E. Kohn, D. Perera, R. Lorek, S. Lambright, M. Imboden and M. Zamkov, *J. Vis. Exp.,* 2012, **66**, e4296.
[68] N. Kholmicheva, N. Razgoniaeva, P. Yadav, A. Lahey, C. Erickson, P. Moroz, D. Gamelin and M. Zamkov, *J. Phys. Chem. C*, 2017, **121**, 1477
[69] T. Franzl, T. A. Klar, S. Schietinger, A. L. Rogach and J. Feldmann, *Nano Lett.,* 2004, **4**, 1599.
[70] F. Xu, X. Ma, C. R. Haughn, J. Benavides, M. F. Doty and S. G. Cloutier, *ACS Nano*, 2011, **5**, 9950
[71] C. Weerd, L. Gomez, H. Zhang, W. J. Buma, G. Nedelcu, M. V. Kovalenko and T. Gregorkiewicz, *J. Phys. Chem. C,* 2016, **120**, 13310.
[72] M. Yuan, L. N. Quan, R. Comin, G. Walters, R. Sabatini, O. Voznyy, S. Hoogland, Y. Zhao, E. M. Beauregard, P. Kanjanaboos, Z. Lu, D. H. Kim and E. H. Sargent, *Nat. Nanotechnol.,* 2016, **11**, 872
[73] J. Y. Kim, V. Adinolfi, B. R. Sutherland, O. Voznyy, S. J. Kwon, T. W. Kim, J. Kim, H. Ihee, K. Kemp, M. Adachi, M. Yuan, I. Kramer, D. Zhitomirsky, S. Hoogland and E. H. Sargent, *Nat. Commun.,* 2015, **6**, 7772.
[74] V. I. Klimov, *Annu. Rev. Phys. Chem.,* 2007, **58**, 635
[75] V. I. Klimov, A. A. Mikhailovsky, S. Xu, A. Malko, J. A. Hollingsworth, C. A. Leatherdale, H. Eisler and M. G. Bawendi, *Science,* 2000, **290**, 314.

[76] Z. Yang, M. Pelton, I. Fedin, D. V. Talapin and E. Waks, *Nat. Commun.,* 2017, **8**, 1.
[77] Y. Yan, R. W. Crisp, J. Gu, B. D. Chernomordik, G. F. Pach, A. R. Marshall, J. A. Turner and M. C. Beard, *Nat. Energy,* 2017, **2**, 17052.
[78] M. Zamkov, *Nat. Energy,* 2017, **2**, 17072
[79] J. P. Philbin and E. Rabani, *Nano Lett.,* 2018, **18**, 7889
[80] F. García-Santamaría, Y. Chen, J. Vela, R. D. Schaller, J. A. Hollingsworth and V. I. Klimov, *Nano Lett.,* 2009, **9**, 3482.
[81] Y. Park, J. Lim, N. S. Makarov and V. I. Klimov, *Nano Lett.,* 2017, **17**, 5607.
[82] F. T. Rabouw, P. Lunnemann, van Dijk-Moes, Relinde J A, M. Frimmer, F. Pietra, A. F. Koenderink and D. Vanmaekelbergh, *Nano Lett.,* 2013, **13**, 4884.
[83] P. D. Cunningham, J. E. Boercker, E. E. Foos, M. P. Lumb, A. R. Smith, J. G. Tischler and J. S. Melinger, *Nano Lett.,* 2011, **11**, 3476.
[84] L. A. Padilha, J. T. Stewart, R. L. Sandberg, W. K. Bae, W. Koh, J. M. Pietryga and V. I. Klimov, *Nano Lett.,* 2013, **13**, 1092.
[85] M. Zavelani-Rossi, M. G. Lupo, F. Tassone, L. Manna and G. Lanzani, *Nano Lett.*, 2010, **10**, 3142.
[86] M. Pelton, J. J. Andrews, I. Fedin, D. V. Talapin, H. Leng and S. K. O'Leary, *Nano Lett.,* 2017, **17**, 6900.
[87] C. She, I. Fedin, D. S. Dolzhnikov, A. Demortière, R. D. Schaller, M. Pelton and D. V. Talapin, *Nano Let.,* 2014*, **14, 2772***
[88] Q. Li and T. Lian, *Nano Lett.,* 2017, **17**, 3152.
[89] Y. Park, W. K. Bae, T. Baker, J. Lim and V. I. Klimov, *Nano Lett*., 2015, **15**, 7319.
[90] M. Pelton, *J. Phys. Chem. C,* 2018, **122**, 10659
[91] N. Razgoniaeva, P. Moroz, M. Yang, D. S. Budkina, H. Eckard, M. Augspurger, D. Khon, A. N. Tarnovsky and M. Zamkov, *J. Am. Chem. Soc*., 2017, **139**, 7815.
[92] N. Razgoniaeva, M. Yang, C. Colegrove, N. Kholmicheva, P. Moroz, H. Eckard, A. Vore and M. Zamkov, *Chem. Mater*., 2017, **29**, 7852-7858
[93] B. G. Jeong, Y. Park, J. H. Chang, I. Cho, J. K. Kim, H. Kim, K. Char, J. Cho, V. I. Klimov, P. Park, D. C. Lee and W. K. Bae, *ACS Nano,* 2016, **10**, 9297.
[94] J. Schrier and L-W. Wang, *Phys. Rev. B,* 2006, **73**, 245332.
[95] C.-L. Weng, I-C. Chen and Y.-C. Tsai, *Phys. Rev B,* 2007, **76**, 195313.
[96] S. Ithurria and B. Dubertret, *J. Am. Chem. Soc*., 2008, **130**, 16504.
[97] M. Aerts, T. Bielewicz, C. Klinke, F. C. Grozema, A. J. Houtepen, J. M. Schins and L. D. A. Siebbeles, *Nat. Comm*., 2014, **5**, 3789.
[98] P. Sippel, W. Albrecht, van der Bok, Johanna C, R. Moes, T. Hannappel, R. Eichberger and D. Vanmaekelbergh, *Nano Lett.* 2013, **13**, 1655-1661.
[99] S. Kim, H. Huang, H. E. Pudavar, Y. Cui and P. N. Prasad, *Chem. Mater.,* 2007, **19**, 5650
[100] Y. Park, A. Pravitasari, J. E. Raymond, J. D. Batteas and D. H. Son, *ACS Nano*, 2013, **7**, 10544
[101] W. Zhang, W. Zhuang, X. Xing, B. Xu, D. Wu, H. Liu, K. Wang, R. Liu and X. W. Sun, *J. Mater. Chem. C*, 2018, **6**, 11280
[102] J. Li,S. K. Cushing, F. Meng, T. R. Senty, A. D. Bristow and N. Wu, *Nat. Photonics*, 2015, **9**, 601
[103] N. S. Abadeer, M. R. Brennan, W. L. Wilson and C. J. Murphy, *ACS Nano,* 2014, **8**, 8392.
[104] J. R. Lakowicz, K. Ray, M. Chowdhury, H. Szmacinski, Y. Fu, J. Zhang and K. Nowaczyk, *Analyst,* 2008, **133**, 1308
[105] J. R. Lakowicz, *Anal. Biochem.,* 2005, **337**, 171
[106] S. Khatua, P. Paulo, H. Yuan, A. Gupta, P. P. Zijlstra and M. Orrit, *ACS Nano,* 2014, **8**, 4440-4449.
[107] T. Sen and A. Patra, *J Phys Chem C*, 2012, **116**, 17307−17317.
[108] E. Heydari, I. Pastoriza-Santos, R. Flehr, L. M. Liz-Marzán and J. Stumpe, *J. Phys. Chem. C*, 2013, **117**, 16577
[109] A. P. Demchenko, *Methods Appl. Fluoresc.,* 2013, **1**, 022001.
[110] J. Malicka, I. Gryczynski, Z. Gryczynski and J. R. Lakowicz, *Anal. Biochem.,* 2003, **315**, 57−66.
[111] O.G. Tovmachenko, C. Graf, D. J. van den Heuvel, A. van Blaaderen and H. C. Gerritsen, *Adv. Mater.,* 2006, **18**, 91−95.
[112] S. Y. Lee, K. Nakaya, T. Hayashi and M. Hara, *Phys. Chem. Chem. Phys.*, 2009, **11**, 4403.
[113] J. Seelig, K. Leslie, A. Renn, S. Kühn, V. Jacobsen, M. van de Corput, C. Wyman and V. Sandoghdar, *Nano Lett.*, 2007, **7**, 685.
[114] G. P. Acuna, M. Bucher, I. H. Stein, C. Steinhauer, A. Kuzyk, P. Holzmeister, R. Schreiber, A. Moroz, F. D. Stefani, T. Liedl, F. C. Simmel and P. Tinnefeld, *ACS Nano,* 2012, **6**, 3189
[115] E. Dulkeith, A. Morteani, T. Niedereichholz, T. A. Klar, J. Feldmann, S. A. Levi, F. C. van Veggel, D. N. Reinhoudt, M. Moller and D. I. Gittins, *Phys. Rev. Lett.*, 2002, **89**, 203002.
[116] T. L. Jennings, M. P. Singh and G. F. Strouse, *J. Am. Chem. Soc.*, 2006, **128**, 5462
[117] L. Jiang, J. Qian, X. Li and S. He, *Appl. Phys. Let.*, 2009, **94**, 063111.
[118] P. Reineck, D. Gómez, S. H. Ng, M. Karg, T. Bell, P. Mulvaney and U. Bach, *ACS Nano,* 2013, **7**, 6636
[119] N. S. Abadeer, M. R. Brennan, W. L. Wilson and C. J. Murphy, *ACS nano,* 2014, **8**, 8392
[120] R. Bardhan, N. K. Grady, J. R. Cole, A. Joshi and N. J. Halas, *ACS Nano*, 2009, **3**, 744
[121] Y. Fu, J. Zhang and J. R. Lakowicz, *J. Am. Chem. Soc.,* 2010, **132**, 5540
[122] N. Gandra, C. Portz, L. Tian, R. Tang, B. Xu, S. Achilefu and S. Singamaneni, *Angew. Chem. Int. Ed.,* 2014, **53**, 866
[123] J. Li, C. Li and R. F. Aroca, *Chem. Soc. Rev.,* 2017, **46**, 3962
[124] M. Wang, B. B. Rajeeva, L. Scarabelli, E. P. Perillo, A. K. Dunn, L. M. Liz-Marzán and Y. Zheng, *J. Phys. Chem. C*, 2016, **120**, 14820
[125] S. Park, M. Pelton, M. Liu, P. Guyot-Sionnest and N. F. Scherer, *J. Phys. Chem. C,* 2007, **111**, 116.
[126] C. Sönnichsen, T. Franzl, T. Wilk, G. von Plessen, J. Feldmann, O. Wilson and P. Mulvaney, *Phys. Rev. Lett.,* 2002, **88**, 077402.
[127] T. Zhao, J. W. Jarrett, J. S. Johnson, K. Park, R. A. Vaia and K. L. Knappenberger, *J. Phys. Chem. C*, 2016, **120**, 4071.
[128]C. C. D. Wang, W. C. H. Choy, C. Duan, D. D. S. Fung, W. E. I. Sha, F. Xie, F. Huang and Y. Cao, *J. Mater. Chem.,* 2012, **22**, 1206
[129] X. Chen, L. Zuo, W. Fu, Q. Yan, C. Fan and H. Chen, *Sol. Energy Mater Sol. Cells*, 2013, **111**, 1
[130] H. F. Zarick, O. Hurd, J. A. Webb, C. Hungerford, W. R. Erwin and R. Bardhan, *ACS Photonics,* 2014, **1**, 806
[131] E. S. Arinze, B. Qiu, G. Nyirjesy, and S. M. Thon, *ACS Photonics*, 2016, **3**, 158
[132] D. Paz-Soldan, A. Lee, S. M. Thon, M. M. Adachi, H. Dong, P. Maraghechi, M. Yuan, A. Labelle, S. Hoogland, K Liu, E. Kumacheva and E. H. Sargent, *Nano Lett.*, 2013, **13**, 1502

[133] S. K. Cushing, J. Li, J. Bright, B. T. Yost, P. Zheng, A. D. Bristow and N. Wu, *J. Phys. Chem. C*, 2015, **119**, 16239
[134] S. Chen, Y. Wang, Q. Liu, G. Shi, Z. Liu, K. Lu, L. Han, X. Ling, H. Zhang, S. Cheng and W. Ma, *Adv. Energy Mater.*, 2018, **8**, 1701194
[135] D. T. Gangadharan, Z. Xu, Y. Liu, R. Izquierdo and D. Ma, *Nanophotonics*, 2017, **6**, 153
[136] Y. He, C. Liu, J. Li, X. Zhang, Z. Li, L. Shen, W. Guo, and S. Ruan. *ACS Appl. Mater. Interfaces*, 2015, **7**, 15848
[137] N. Kholmicheva, L. Royo Romero, J. Cassidy and M. Zamkov, *Nanophotonics*, 2018, DOI: 10.1515/nanoph-2018-0143
[138] Y. H. Jang, Y. J. Jang, S. Kim, L. N. Quan, K. Chung and D. H. Kim, *Chem. Rev.,* 2016, **116**, 14982−15034.
[139] J. Nguyen, Y. Ma, T. Luo, R. G. Bristow, D. A. Jaffray and Q. B. Lu, *Proc. Natl. Acad. Sci. U. S. A.*, 2011, **108**, 11778
[140] W. A. Tisdale, K. J. Williams, B. A. Timp, D. J. Norris, E. S. Aydil and X. Y. Zhu, *Science*, 2010, **328**, 1543
[141] K. Ueno, T. Oshikiri, Q. Sun, X. Shi and H. Misawa, *Chem. Rev*., 2018, **118**, 2955−2993.
[142] T. Tatsuma, H. Nishi and T. Ishida, *Chem. Sci.*, 2017, **8**, 3325.
[143] S. K. Cushing, A. D. Bristowa and N. Wu, *Phys. Chem. Chem. Phys.,* 2015, **17**, 30013.
[144] K. P. Acharya, N. N. Hewa-Kasakarage, T. R. Alabi, I. Nemitz, E. Khon, B. Ullrich, P. Anzenbacher and M. Zamkov, *J. Phys. Chem. C*, 2010, **114**, 12496
[145] H. J. Lee, P. Chen, S. J. Moon, F. Sauvage, K. Sivula, T. Bessho, D. R. Gamelin, P. Comte, S. M. Zakeeruddin, S. I. Seok, M. Graetzel and M. K. Nazeeruddin, *Langmuir*, 2009, **25**, 7602
[146] P. K. Santra and P. V. Kamat, *J. Am. Chem. Soc.,* 2013, **135**, 877
[147] A. J. Haring, M. E. Pomatto, M. R. Thornton and A. J. Morris, *ACS Appl. Mater. Interfaces*, 2014, **6**, 15061
[148] J. J. H. Pijpers, R. Koole, W. H. Evers, A. J. Houtepen, S. Boehme, C. de Mello Donegá, D. Vanmaekelbergh, and M. Bonn, *J. Phys. Chem. C*, 2010, **114**, 18866
[149] R. S. Selinsky, Q. Ding, M. S. Faber, J. C. Wright and S. Jin, *Chem. Soc. Rev*., 2013, **42**, 2963
[150] W. Li and X. Zhong, *J. Phys. Chem. Lett.*, 2015, **6**, 796
[151] J. Poppe, S. G. Hickey and A. Eychmüller*, J. Phys. Chem. C*, 2014, **118**, 17123
[152] P. V. Kamat, K. Tvrdy, D. R. Baker and J. G. Radich, *Chem. Rev*., 2010, **110**, 6664
[153] S. V. Kershaw, A. S. Susha and A. L. Rogach, *Chem. Soc. Rev.*, 2013 **42**, 3033
[154] R. M. Clegg, Förster Resonance Energy Transfer—FRET: What Is It, Why Do It, and How It's Done, In *FRET and FLIM Techniques. Laboratory Techniques in Biochemistry and Molecular Biology*, ed. T. W. J. Gadella, Elsevier, Amsterdam, 2009, Vol. 33. pp. 1-57.
[155] A. Periasamy, *J. Biomed. Opt.,* 2001, **6**, 287-291.
[156] I. L. Medintz, T. Pons, K. Susumu, K. Boeneman, A. Dennis, D. Farrell, J. R. Deschamps, J. S. Melinger, G. Bao and H. Mattoussi, *J. Phys. Chem. C*, 2009, **113**, 18552.
[157] A. Kapur, F. Aldeek, X. Ji, M. Safi, W. Wang, A. D. Cid, O. Steinbock and H. Mattoussi, *Bioconjugate. Chem.,* 2017, **28**, 678.
[158] Q. Ma and X. Su, *Analyst,* 2011, **136**, 4883.
[159] L. Stryer and R. P. Haugland, *Proc. Natl. Acad. Sci. U. S. A.,* 1967, **58**, 719.
[160] L. Stryer, *Annu. Rev. Biochem.,* 1978, **47**, 819.
[161] S. Preus and L. M. Wilhelmsson, *ChemBioChem,* 2012, **13**, 1990.
[162] I. H. Stein, V. Schüller, P. Böhm, P. Tinnefeld and T. Liedl, *ChemPhysChem,* 2011, **12**, 689−695.
[163] B. P. Aryal and D. E. Benson, *J. Am. Chem. Soc.,* 2006, **128**, 15986.
[164] A. Boulesbaa, Z. Huang, D. Wu and T. Lian, *J. Phys. Chem. C,* 2010, **114**, 962.
[165] A. Boulesbaa, A. Issac, D. Stockwell, Z. Huang, J. Huang, J. Guo and T. Lian, *J. Am.Chem. Soc.,* 2007, **129**, 15132.
[166] D. Perera, R. Lorek, R. S. Khnayzer, P. Moroz, T. O'Connor, D. Khon, G. Diederich, E. Kinder, S. Lambright, F. N. Castellano and M. Zamkov, *J. Phys. Chem. C*, 2012, **116**, 22786.
[167] P. Moroz, N. Razgoniaeva, Y. He, G. Jensen, H. Eckard, H. P. Lu and M. Zamkov, *ACS Nano*, 2017, **11**, 4191
[168] N. J. Thompson, M. W. B. Wilson, D. N. Congreve, P. R. Brown, J. M. Scherer, T. S. Bischof, M. Wu, N. Geva, M. Welborn, T. V. Voorhis, V. Bulović, M. G. Bawendi and M. A. Baldo, *Nat. Mater.,* 2014, **13**, 1039.
[169] M. Tabachnyk, B. Ehrler, S. Gélinas, M. L. Böhm, B. J. Walker, K. P. Musselman, N. C. Greenham, R. H. Friend and A. Rao, *Nat. Mater.,* 2014, **13**, 1033.
[170] C. Mongin, S. Garakyaraghi, N. Razgoniaeva, M. Zamkov and F. N. Castellano, *Science,* 2016, **351**, 369.
[171] M. Wu, D. N. Congreve, M. W. B. Wilson, J. Jean, N. Geva, M. Welborn, T. V. Voorhis, V. Bulović, M. G. Bawendi and M. A. Baldo, *Nat. Photonics,* 2016, **10**, 31.
[172] S. Garakyaraghi and F. N. Castellano, *Inorg. Chem.*, 2018, **57**, 2351
[173] Z. Huang and M. L. Tang, *J. Phys. Chem. Lett.*, 2018, **9**, 6198
[174] L. Nienhaus, M. Wu, N. Geva, J. J. Shepherd, M. W. B. Wilson, V. Bulović, T. V. Voorhis, M. A. Baldo and M. G. Bawendi, *ACS Nano*, 2017, **11**, 7848
[175] L. Nienhaus, M. Wu, V. Bulović, M. A. Baldo and M. G. Bawendi, *Dalton Trans.*, 2018, **47**, 8509
[176] X Li, Z. Huang, R. Zavala and M. L. Tang, *J. Phys. Chem. Lett.,* 2016, **7**, 1955
[177] J. A. Bender, E. K. Raulerson, X. Li, T. Goldzak, P. Xia, T. V. Voorhis, M. L. Tang, S. T. Roberts, *J. Am. Chem. Soc.*, 2018, **140**, 7543
[178] A. L. Efros, M. Rosen, M. Kuno, M. Nirmal, D. J. Norris and M. Bawendi, *Phys. Rev. B*, 1996, **54**, 4843
[179] G. D. Scholes, *Adv. Funct. Mater.*, 2008, **18**, 1157
[180] N. Kholmicheva, P. Moroz, H. Eckard, G. Jensen and M. Zamkov, *ACS Energy Lett.*, 2017, **2**, 154
[181] K. V. Reich and B. I. Shklovskii, *ACS Nano,* 2016, **10**, 10267.
[182] R. C. Powell and Z. G. Soos, *J. Lumin*., 1975, **11**, 1-45.
[183] G. M. Akselrod, P. B. Deotare, N. J. Thompson, J. Lee, W. A. Tisdale, M. A. Baldo, V. M. Menon and V. Bulović, *Nat. Commun*., 2014, **5**, 3646.
[184] S. J. Yoon, Z. Guo, P. C. dos Santos Claro, E. V. Shevchenko and L. Huang, *ACS Nano,* 2016, **10**, 7208.
[185] R. H. Gilmore, E. M. Y. Lee, M. C. Weidman, A. P. Willard and W. A. Tisdale, *Nano Lett.*, 2017, **17**, 893
[186] M. S. Azzaro, A. Dodin, D. Y. Zhang, A. P. Willard and S. T. Roberts, *Nano Lett.*, 2018, **18**, 3259
[187] A. H. Proppe, J. Xu, R. P. Sabatini, J. Z. Fan, B. Sun, S. Hoogland, S. O. Kelley, O. Voznyy and E. H. Sargent, *Nano Lett.*, 2018, **18**, 7052
[188] E. M. Y. Lee and W. A. Tisdale, *J. Phys. Chem. C,* 2015, **119**, 9005.

[189] C. R. Kagan, C. B. Murray, M. Nirmal and M. G. Bawendi, *Phys. Rev. Lett.,* 1996, **76**, 1517.
[190] S. A. Crooker, J. A. Hollingsworth, S. Tretiak and V. I. Klimov, *Phys. Rev. Lett.,* 2002, **89**, 186802 .
[191] F. Xu, X. Ma, C. R. Haughn, J. Benavides, M. F. Doty and S. G. Cloutier, *ACS Nano,* 2011, **5**, 9950.
[192] T. Franzl, D. S. Koktysh, T. A. Klar, A. L. Rogach, J. Feldmann and N. Gaponik, *Appl. Phys. Lett.,* 2004, **84**, 2904.
[193] J. Miyazaki and S. Kinoshita, *J. Phys. Soc. Jpn*., 2012, **81**, 074708
[194] J. Miyazaki and S. Kinoshita, *Phys. Rev. B*, 2012, **86**, 035303.
[195] J. Zhang, J. Tolentino, E. R. Smith, J. Zhang, M. C. Beard, A. J. Nozik, M. Law and J. C. Johnson, *J. Phys. Chem. C*, 2014, **118**, 16228
[196] J. Gao, J. Zhang, J. van de Lagemaat, J. C. Johnson and M. C. Beard, *ACS Nano*, 2014, **8**, 12814
[197] G. M. Akselrod, F. Prins, L. V. Poulikakos, E. M. Y. Lee, M. C. Weidman, A. J. Mork, A. P. Willard, V. Bulović and W. A. Tisdale, *Nano Lett.*, 2014, **14**, 3556
[198] N. Hildebrandt, How to Apply FRET: From Experimental Design to Data Analysis, in *FRET - Förster Resonance Energy Transfer. From Theory to Applications,* ed. I. L. Medintz, and N. Hildebrandt, N., Wiley-VCH, Weinheim, Germany, 2014, pp 105−156
[199] P. T. Snee, R. C. Somers, G. Nair, J. P. Zimmer, M. G. Bawendi and D. G. Nocera, *J. Am. Chem. Soc.,* 2006, **128**, 13320.
[200] I. L. Medintz and H. Mattoussi, *Phys. Chem. Chem. Phys.,* 2008, **11**, 17.
[201] I. Yildiz, M. Tomasulo and F. M. Raymo, *Proc. Natl. Acad. Sci. U. S. A.,* 2006, **103**, 11457.
[202] I. L. Medintz, T. Pons, S. A. Trammell, A. F. Grimes, D. S. English, J. B. Blanco-Canosa, P. E. Dawson and H. Mattoussi, *J. Am. Chem. Soc.,* 2008, **130**, 16745.
[203] M. Sykora, M. A. Petruska, J. Alstrum-Acevedo, I. Bezel, T. J. Meyer and V. I. Klimov, *J. Am. Chem. Soc.,* 2006, **128**, 9984.
[204] I. Yildiz, E. Deniz and F. M. Raymo, *Chem. Soc. Rev.,* 2009, **38**, 1859.
[205] P. Moroz, N. Razgoniaeva, A. Vore, H. Eckard, N. Kholmicheva, A. McDarby, A. O. Razgoniaev, A. D. Ostrowski, D. Khon and M. Zamkov, *ACS Photonics,* 2017, **4**, 2290.
[206] P. Moroz, W. P. Klein, K. Akers, A. Vore, N. Kholmicheva, N. Razgoniaeva, D. Khon, S. A. Díaz, I. L. Medintz and M. Zamkov, *J. Phys. Chem. C,* 2017, **121**, 26226.
[207] P. Moroz, Z. Jin, Y. Sugiyama, D. Lara, N. Razgoniaeva, M. Yang, N. Kholmicheva, D. Khon, H. Mattoussi and M. Zamkov, *ACS Nano*, 2018, **12**, 5657
[208] D. M. Arias-Rotondo and J. K. McCusker, *Chem. Soc. Rev.,* 2016, **45**, 5803
[209] M. Hara, C. C. Waraksa, J. T. Lean, B. A. Lewis and T. E. Mallouk, *J. Phys. Chem. A,* 2000, **104**, 5275
[210] P. Moroz, A. Boddy and M. Zamkov, *Front. Chem.*, 2018, **6**, 353
[211] W. W. Yu, L. Qu, W. Guo and X. Peng, *Chem. Mater.,* 2003, **15**, 2854
[212] R. E. Blankenship, *Molecular mechanisms of photosynthesis*, Wiley-Blackwell, 2013.
[213] M. M. Najafpour, S. Heidari, S. E. Balaghi, M. Holynska, M. H. Sadr, B. Soltani, M. Khatamian, A. W. Larkum and S. I. Allakhverdiev, *Biochim. Biophys. Acta, Bioenerg*., 2017, **1858**, 156.
[214] S. Ye, R.-T. Chen, Y.-X. Xu, F.-T. Fan, P.-W. Du, F.-X. Zhang, X. Zong, T. Chen, Y. Qi, P. Chen, Z. Chen and C. Li, *J. Catal.*, 2016, **338**, 168
[215] S. Ye, C. Ding, R.-T. Chen, F.-T. Fan, P. Fu, H. Yin, X. Wang, Z. Wang, P.-W. Du, and C. Li, *J. Am. Chem. Soc.*, 2018, **140**, 3250
[216] M. S. Kodaimati, S. Lian, G. C. Schatz and E. A. Weiss, *Proc. Natl. Acad. Sci. U. S. A.,* 2018, **115**, 8290.
[217] C. Liu, B. C. Colón, M. Ziesack, P. A. Silver and D. G. Nocera, *Science,* 2016, **352**, 1210
[218] N. Rotenberg and L. Kuipers, *Nat. Photonics,* 2014, **8**, 919.
[219] L. Sun, B. Bai and J. Wang, *Opt. Express,* 2018, **26**, 18644.
[220] M. Wagner, Z. Fei, A. S. McLeod, A. S. Rodin, W. Bao, E. G. Iwinski, Z. Zhao, M. Goldflam, M. Liu, G. Dominguez, M. Thiemens, M. M. Fogler, A. H. Castro Neto, C. N. Lau, S. Amarie, F. Keilmann and D. N. Basov, *Nano Lett.,* 2014, **14**, 894.